Redox Biology 13 (2017) 39–59

Contents lists available at ScienceDirect

Redox Biology

journal homepage: www.elsevier.com/locate/redox

Review article

Direct $^1O_2$ optical excitation: A tool for redox biology

Alfonso Blázquez-Castro[a,b,*]

[a] Department of Physics of Materials, Faculty of Sciences, Autonomous University of Madrid, Madrid, Spain
[b] Formerly at Aarhus Institute of Advanced Studies (AIAS)/Department of Chemistry, Aarhus University, Aarhus, Denmark

ARTICLE INFO

Keywords:
Singlet oxygen
Reactive Oxygen Species (ROS)
Redox biology
Biophotonics
Low-level laser therapy (LLLT)
Photodynamic therapy (PDT)

ABSTRACT

Molecular oxygen (O_2) displays very interesting properties. Its first excited state, commonly known as singlet oxygen ($^1O_2$), is one of the so-called Reactive Oxygen Species (ROS). It has been implicated in many redox processes in biological systems. For many decades its role has been that of a deleterious chemical species, although very positive clinical applications in the Photodynamic Therapy of cancer (PDT) have been reported. More recently, many ROS, and also $^1O_2$, are in the spotlight because of their role in physiological signaling, like cell proliferation or tissue regeneration. However, there are methodological shortcomings to properly assess the role of $^1O_2$ in redox biology with classical generation procedures. In this review the direct optical excitation of O_2 to produce $^1O_2$ will be introduced, in order to present its main advantages and drawbacks for biological studies. This photonic approach can provide with many interesting possibilities to understand and put to use ROS in redox signaling and in the biomedical field.

1. Introduction

As presented in the enlightening and seminal book “Oxygen: The molecule that made the world” by Lane [1], molecular oxygen (O_2) is a fascinating compound. This element has shaped the Earth at many levels, from the geophysical one to the atmosphere and living entities. Its build-up in the atmosphere around 2.7-2.3 billion years ago triggered what has probably been the most devastating biological crisis and extinction event the Earth has witnessed. Once oxygen had accumulated in sufficient quantities, living organisms adapted to it, some of them even “learning” how to use it to further oxidize reduced compounds to obtain much more energy.

With this oxygen incorporation to the metabolic network of living cells, it came as no surprise that oxygen, and its partly reduced chemical products known as Reactive Oxygen Species (ROS), also assumed regulating and signaling roles [2]. This signaling role has only recently started to be acknowledged by the scientific community, in what is becoming a new branch of biology known as Redox Biology [3–5]. Within this field, the deleterious effects of ROS, whenever they are produced in too large quantities or at inappropriate times/places in living organisms, are also explored to provide answers to many disorders and diseases that have their origin in a redox deregulation of cell physiology.

Currently, the physiological and pathological role of ROS is a very fast growing area. In this review I will focus in one of these ROS, in particular singlet oxygen ($^1O_2$). Even within this reactive species, a whole range of articles and reviews already exist ([6–10] to name a few reviews), as it is usually invoked as the main cytotoxic compound involved in the clinical therapeutic approach known as Photodynamic Therapy (PDT) [11–15]. However, it has turned out that $^1O_2$, as it happens with many other ROS, is also involved in physiological cellular processes [2,16–18], and/or modulates the cellular redox potential in such a way as to induce those processes [19–21]. As such, the study of $^1O_2$ both as a biological damaging compound as well as a cellular signaling agent is of utmost importance. Classically, $^1O_2$ has been generated in living systems employing a photodynamic approach (see Section 2.2 for more details on this). Recently, however several groups have re-sparked interest on the possibility to *directly* excite the oxygen molecule with light at certain wavelengths, for biological research or clinical applications [22]. Some successful light wavelengths employed towards this end have been 1270 nm [23–28], 1065 nm [29–31] and 760 nm [32–34], to name a few. However, it must be mentioned (see details in Section 4) that research on the direct optical excitation of O_2 predates by several decades these studies.

In this review I will present and elaborate on the different optical wavelength regions to directly excite O_2 with light. First, I will briefly introduce the excited states of molecular oxygen, and their classical excitation approaches (Section 2). Then, an introduction to the biological action of $^1O_2$ will be provided (Section 3). In Section 4 the available spectral regions to directly excite O_2 for biological purposes

* Correspondence address: Department of Physics of Materials, Faculty of Sciences, C/Francisco Tomás y Valiente 7, Autonomous University of Madrid, Cantoblanco 28049, Madrid, Spain.
E-mail address: singlet763@gmail.com.

http://dx.doi.org/10.1016/j.redox.2017.05.011
Received 7 April 2017; Received in revised form 30 April 2017; Accepted 20 May 2017
Available online 25 May 2017

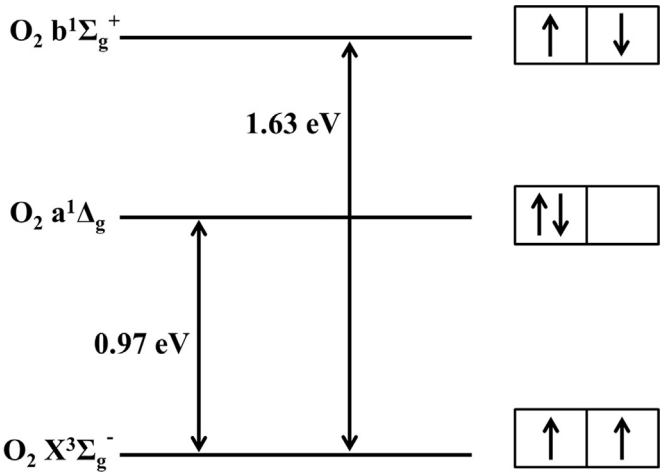

Fig. 1. Electronic states of the oxygen molecule. The fundamental (O_2 $X^3\Sigma_g^-$) and the two lowest electronic excited states of molecular oxygen (O_2 $a^1\Delta_g$ and O_2 $b^1\Sigma_g^+$) are shown in the scheme. The fundamental, or ground, state is a triplet, while the two excited levels are singlets. The energy gap between the fundamental level and the other two levels is shown in eV. To the right, a simplified scheme of the different electronic arrangement featured by each electronic level. The boxes represent electronic orbitals, and the arrows the electronic spins.

will be detailed, with emphasis on their advantages and drawbacks. Finally, an outlook on different established or currently under development research areas that can take advantage of this photonic approach will be delineated (Section 5). It must be stressed that this review will deal with the available photonic options to excite O_2, with redox biology studies in mind. It will only tangentially deal with the proper redox biology and chemistry of $^1O_2$ (many different and excellent reviews have already been published on these topics and they will be cited whenever appropriate).

2. Singlet oxygen

The oxygen molecule O_2 displays some very particular features. Being the second most electronegative element in the periodic table, it would be expected that O_2 is to be a very reactive chemical compound. As it turns out, however, it is a quite unreactive molecule. A testimony to this is the fact that we live in a planet with a 21% oxygen atmospheric content, and nevertheless life thrives and even depends on it. Thus, I will briefly introduce the special characteristics of O_2. From this starting point it will be quite straightforward to understand how O_2 becomes electronically excited and, by extension, which are the main features of the first excited state commonly known as singlet oxygen ($^1O_2$), the topic of this review.

2.1. Basic physical-chemical features of $^1O_2$

The reason why O_2 is so unreactive, in spite of its electronegativity, is the fact that in the fundamental state it assumes a triplet electronic configuration [8–10,35,36]. The way in which the valence electrons arrange in O_2 is such that the configuration with the least energy, has the two outermost electrons in different antibonding orbitals, but with the same spin (see Fig. 1). According to the molecular orbital theory, this arrangement has a triplet character. In formal spectroscopic nomenclature the ground state of O_2 is designed as O_2 $X^3\Sigma_g^-$ [10,35]. A less formal designation is $^3O_2$, stressing the triplet character of the ground state. This ground state has a biradical chemical character, which makes it quite unreactive to most chemical compounds [35,36]. At the same time, this triplet character makes ground state O_2 a paramagnetic compound, where oxygen tends to move to the point of strongest magnetic field.

Increasing in energy, the next two electronic levels of O_2 are of singlet character. This is due to the rearrangement of the electron spin and orbital occupancy (Fig. 1). A certain amount of energy (~ 0.96 eV) is needed to flip one of the electron´s spin. Now, according to selection rules, both electrons can occupy the same orbital by coupling their spins. This first excited O_2 level is designed as O_2 ($a^1\Delta_g$), $^1O_2$ (a) or simply $^1O_2$ [10,35]. A further increase in energy, to 1.62 eV above the ground level, maintains opposite electronic spins, thus singlet in character, but the two electrons again occupy different orbitals. This more energetic state is known as O_2 ($b^1\Sigma_g^+$) or $^1O_2$ (b) [10,35], and it is also a singlet oxygen state. To simplify the nomenclature, and given the biological focus of this review, from this point on I will refer to ground state oxygen (O_2 $X^3\Sigma_g^-$) simply as $^3O_2$, the first singlet excited state -O_2 ($a^1\Delta_g$)- as $^1O_2$, and to the second singlet excited state - O_2 ($b^1\Sigma_g^+$)- as $^1O_2$ (b). The second excited state $^1O_2$ (b) converts very fast (~ picoseconds) to the first excited state $^1O_2$ [6,37], especially in condensed matter (e.g. aqueous solutions), by transforming part of its electronic excitation energy into vibrational oscillations. Therefore, for most singlet oxygen applications in biology, the production of $^1O_2$ (b) can be interpreted as if $^1O_2$ had been directly produced instead. Many optical excitation bands that will be introduced later in this review (Section 4) produce $^1O_2$ (b) in the first place, but this is very quickly transformed into $^1O_2$ in biological systems.

Once produced $^1O_2$ is several orders of magnitude more reactive than $^3O_2$. This is a consequence of the molecule now having a singlet character, which makes it possible for it to interact more efficiently with most chemical compounds [2,36,38–40]. Most commonly, $^1O_2$ reacts with other compounds by producing endoperoxides in the first place. These can further lead to generation of radicals, ROS, peroxides, aldehydes, etc. Most previous biological studies, studying the interaction between $^1O_2$ and biological substrates, have focused on the deleterious reactions that $^1O_2$ drives, which upset the smooth biochemistry of living systems. As it will be presented below, a new paradigm is emerging in which $^1O_2$ can, under the right conditions, regulate physiological cell functions [16,21,33,41–43]. Some of the prevalent reactions of $^1O_2$ with biological substrates will be described in Section 3.

An important feature of $^1O_2$ to consider in biological studies is its lifetime. This is the time it takes for a certain amount of $^1O_2$ to decay to some fraction of its original concentration. As an excited species, $^1O_2$ is in a metastable state: it decays to a lower energy state sooner or later. This decay can occur through different deactivation channels (Fig. 2). The simplest deactivation channel is for $^1O_2$ to emit a photon and reach the fundamental state. As the initial and final electronic states are of different multiplicity (singlet vs. triplet), the light emission is termed phosphorescence. The emission is in a relatively narrow band centered at 1270 nm [6,35,36]. This radiative transition is forbidden by several electromagnetic and quantum mechanical rules [8]. As such, it takes a long time for it to happen in an undisturbed $^1O_2$ molecule. However, in the condensed phase, the deactivation probability increases due to interaction and perturbations by nearby molecules or atoms, and the lifetime is reduced orders of magnitude. This 1270 nm emission is the counterpart of one of the absorption bands of $^3O_2$ that are the main topic of this review (see Section 4.2).

The main deactivation pathway in water and aqueous solutions is physical quenching by internal conversion to the ground state (Fig. 2). This non-radiative transition takes place spontaneously, competing with light emission at 1270 nm. In condensed media, its occurrence is greatly enhanced due to solvent or solute interaction [44]. The key aspect is that $^1O_2$ deactivation takes place without a net chemical reaction. The excitation energy is lost to the medium first as vibrational energy, which finally decays to heat. The energy coupling among $^1O_2$ and apolar non-hydrogenated solvents is much less efficient, and its lifetime is consequently prolonged, reaching very high values (milliseconds) [44–46]. Finally, $^1O_2$ can engage in chemical reactions with a host of substrates. Some important examples directly related to biochemical and biological systems will be presented in Section 3.1.

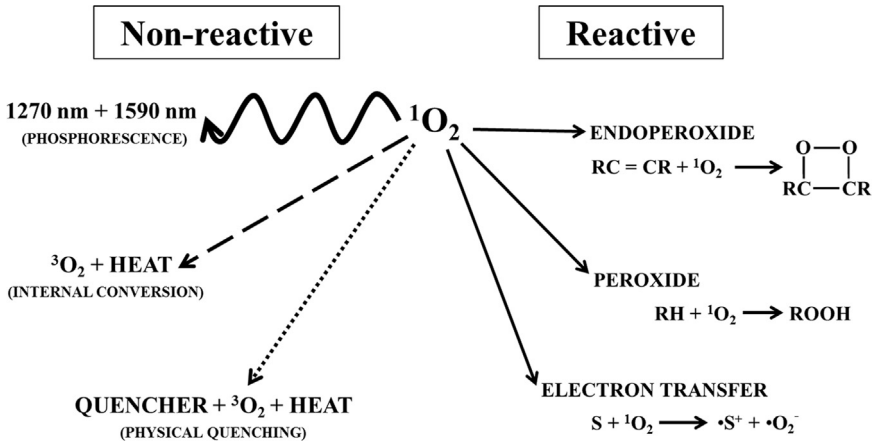

Fig. 2. Radiative and non-radiative deactivation pathways of $^1O_2$. The excited $^1O_2$ can undergo deactivation through different pathways, non-reactive (left) and reactive (right). It can experience a radiative transition to the ground state, emitting a phosphorescent photon at 1270 nm or 1590 nm. It can transform the electronic excitation energy directly to vibration and, eventually, heat. This can happen without external influence (internal conversion) or through environmental interactions with other compounds (physical quenching), like a solvent (*e.g.* H_2O). $^1O_2$ can engage in chemical reactions (reactive branch). Three prototypical kinds of reactions are shown: endoperoxide formation (top), peroxide formation (middle), and electron transfer (bottom). In the scheme R: chemical substituent, C: carbon atom, H: hydrogen atom, S: reduced substrate.

Usually the lifetime is expressed as the time it takes for a given $^1O_2$ population to decay by 1/e (to ~36.78% of the initial amount) [47,48]. The lifetime is highly variable (from 10^{-6} s to 10^3 s), and depends on different environmental parameters, like solvent, solvent phase (gas vs. condensed), temperature, polarity, hydrophobicity, etc [6]. Water happens to be one of the less "$^1O_2$-friendly" solvents. This is due to the very high coupling among the electronic excitation of $^1O_2$ and the vibrational levels of the H_2O molecule. In consequence, the most probable deactivation pathway for $^1O_2$ in H_2O is vibrational dissipation of energy, which quickly decays to heat [6,48]. In aqueous solutions, which obviously are the medium of interest in biological systems, $^1O_2$ lifetime is ~4 μs (Fig. 3) [47,48]. This relatively short lifetime allows $^1O_2$ to diffuse only a small distance from its inception spot. This diffusion distance has been calculated as ~100–150 nm during one lifetime [47,48]. Thus, we would expect a relatively large spatial control over the "sphere of biological action" of $^1O_2$ if we can produce $^1O_2$ in a small enough volume. This topic will be elaborated further in Section 5.1. As ubiquitous as H_2O is in living cells, some structures and organelles have a different composition (e.g. lipid membranes). As a consequence, $^3O_2$ concentration and $^1O_2$ lifetime can be considerably enhanced in those regions and, by extension, chemical/biological activity. These are parameters to be taken into account when $^1O_2$ is generated in or close to those structures [34].

A procedure to extend $^1O_2$ lifetime and its activity sphere is to introduce heavy water (D_2O) in a living system. D_2O vibrational levels are slightly different from those of H_2O. This is, nevertheless, enough to reduce energy transfer from $^1O_2$ to D_2O vibrational levels. As a result, $^1O_2$ lifetime in pure D_2O increases to ~68 μs and diffusion distance to ~500–600 nm [47,48]. On the other hand, D_2O is toxic for cells in the long term, but a compromise concentration of 25% − 50% D_2O in H_2O can be employed in experiments, which preserve cell viability enough to obtain relevant results. In fact, the use of D_2O is a reliable method to prove $^1O_2$ involvement in biological responses, as it will be explained in more detail in Section 5.1.

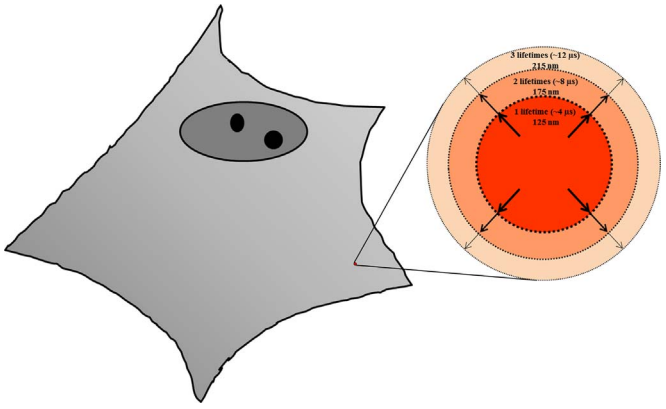

Fig. 3. Diffusion distance of $^1O_2$ in a cell. A prototypical eukaryotic adherent cell is shown to the left. A certain amount of $^1O_2$ is initially produced in the indicated spot. Once produced, $^1O_2$ can diffuse a certain distance before being deactivated by one of the mechanisms presented in Fig. 2. Taken together, they combine to limit the distance $^1O_2$ can diffuse, which is displayed in the magnified circles to the right. The diffusion distances are correlated with the time it takes for oxygen to cover those (lifetimes). Therefore, if $^1O_2$ is carefully produced within a constrained subcellular location (*e.g.* by a laser beam), it will initially perturb only a small cellular volume, offering interesting opportunities to assess biological action mechanisms. (Lifetimes and diffusion distances adapted from [48]).

2.2. Classical excitation mechanisms of $^1O_2$

The classical mechanisms of $^1O_2$ excitation will now briefly be presented. In this way, the reader will be able to better appreciate the advantages and drawbacks of the direct optical excitation of $^1O_2$, to be introduced in Section 4. One of the most common approaches is to employ a compound that transfers electronic excitation energy to $^3O_2$. This compound is known as a photosensitizer (PS). When a PS is excited with light, it becomes electronically excited and can transfer this energy to the $^3O_2$ molecule, under the right circumstances. It would be too lengthy to go into detail about this process, as it is outside the scope of this review. However, the interested reader is directed to some comprehensive publications in the literature on this topic [6–10,12]. Suffice it to say that commonly employed PSs absorb light, from the near ultraviolet (near-UV) through the visible to the near infrared (NIR). These compounds show a relatively long excited state lifetime, which allows them to efficiently interact with $^3O_2$ and transfer their energy to it. However, many PSs have drawbacks in greater or lesser degree when it comes to their incorporation or interaction with living systems (poor uptake, undesirable cell localization, induction of cell stress or straight cytotoxicity, etc.). For certain studies and applications, it can be desirable to excite $^3O_2$ in other ways.

Several methodologies, variants of the classical light-PS photosensitized generation of $^1O_2$, are currently in different developmental stages to deal with some of these drawbacks. The use of genetically-encoded PSs is gaining widespread use. In this approach cells are genetically-directed to synthesize a protein that harbors a PS (modified GFP or

other proteins like the recently reported miniSOG) [49]. Under light excitation, these proteins generate ROS, one of them $^1O_2$. This variant offers a large amount of control as to the subcellular PS localization [33,34]. Given the short intracellular range of $^1O_2$ mentioned in the previous paragraph, the precise positioning of a protein-PS within a certain cellular structure provides a great deal of control in regards to the biology of ROS. Among its drawbacks are the non-negligible interference with endogenous DNA, RNA and protein networks, the limited control over the precise protein-PS localization (for the moment), and the production of different ROS, not restricted to $^1O_2$, during irradiation [33,34].

A second variant to increase control over $^1O_2$ production is the use of non-linear excitation of PSs. It also makes use of a conventional PS, which often has been selected according to its high two-photon absorption. By increasing the exciting light flux rate over the studied area, employing pulsed lasers, the PS absorbs two long-wavelength photons, whose combined energies allow the PS to reach an excited electronic state [10]. Once this happens, the usual energy transfer to $^3O_2$ can take place, leading to $^1O_2$ generation. Two-photon excitation depends critically on the light flux rate, and as a consequence only a focused spot of light is available for PS non-linear excitation. This leads to a very high spatial resolution for the $^1O_2$ source spot (< 1 μm), which is certainly an asset in experiments done at the single cell level [33,34]. However, its application is very limited when it comes to a larger target (e.g. organ or whole animal), and it usually happens that good two-photon absorbing PSs have other undesirable biological constrains, like inadequate cellular uptake. A very recent development of non-linear absorption-sensitized $^1O_2$ generation is the pulsed excitation of metal or semiconductor nanoparticles, leading to the so-called hot-electron excitation [50,51]. Briefly, a very short laser pulse (femtoseconds) excites a small population of electrons in the nanoparticle by plasmon resonance. These excited electrons gain a fairly large amount of energy (few eV). Before they thermalize (100 fs-1ps), they can engage in high-energy chemistry with compounds adsorbed at the nanoparticle´s surface, like $^3O_2$ molecules, for example [52]. So, $^1O_2$ is generated at the interface between nanoparticle and medium. As fascinating as this approach is, it is necessary to introduce the nanoparticles into the living system under study. And then, a fs-pulsed laser source is mandatory for the excitation mechanism to work. These considerations make this methodology useful only for certain experimental conditions, and probably will not become a widespread technique to study the biological role of $^1O_2$.

A quite successful $^1O_2$ production approach is the use of dark chemical reactions, in which light is unnecessary to achieve oxygen excitation. This is possible because certain highly exothermic reactions make enough free energy available to efficiently excite $^3O_2$ [35,36,40]. The reaction produces some excited state product, that collides with $^3O_2$ and transfers the excitation energy, after which $^1O_2$ is obtained. Unfortunately, most chemical reactions producing $^1O_2$ either require very reactive reagents and/or produce very reactive intermediates (e.g. classical reaction between hydrogen peroxide and hypochlorite). These chemical compounds are commonly incompatible with living systems, as they directly damage them. It is worth mentioning, however, that certain biochemical systems [17,53] and cells [17,54,55] do indeed take advantage of some dark reactions to produce $^1O_2$ without need of light. If this production has relevant biological roles, as it seems to, or they occur as a side effect and have a generic deleterious outcome, is not yet clear [2,17]. More details on this will be provided in Section 3.

A particular class of chemical $^1O_2$ sources deserves mentioning at this point. These are endoperoxides of organic molecules that form when the organic precursors interact with $^1O_2$ [35,56,57]. The $^1O_2$ becomes “stored” in the endoperoxide in a kind of latent state. Later, when these endoperoxides are exposed to higher temperatures or light, they release the $^1O_2$ which then diffuses into the surroundings. By modulating the releasing parameter (commonly increasing the temperature), the biological action of $^1O_2$ can be studied [16,58,59]. Advantages of this methodology are the relatively sharp control of the total amount of $^1O_2$ released and the certainty that the only ROS generated in the first place is $^1O_2$. A big issue can be the uptake/interaction of the endoperoxide with cells, and the cytotoxicity of these compounds per se (these organic compounds show aromatic portions which can, for example, lead to nucleic acid intercalation). All in all, they are a nice approach to the study of the biological impact of $^1O_2$, although few publications report on their use towards this goal.

3. Redox biology of $^1O_2$

Here, a brief introduction to the basic chemistry and biological action of $^1O_2$ will be presented. The aim is to sketch the current knowledge in this area, so that the advantages and opportunities, as well as some of the drawbacks, which direct optical excitation of $^1O_2$ offers, can be better understood and appreciated.

3.1. Redox chemistry

The chemistry of $^1O_2$ is dominated, as would be expected, by a strong oxidative behavior. Most commonly, the first reaction step with organic compounds is the establishment of a peroxide intermediate [10,38]. Then, radical species (R-O•) are produced, as the RO-OR bond is quite labile. From this point on, radical reactions propagate easily, in many cases involving $^3O_2$ given that it readily engages in reactions with radicals. Therefore, even when the first reaction steps usually narrow down to the generation of peroxides, secondary reactions rapidly widen the available reacting species. Among these one can find organic radicals (-R•), organic alkoxyl radicals (R-O•), organic peroxyl radicals (R-O-O•), organic hydroperoxides (R-O-OH), superoxide ($•O_2^-$), hydrogen peroxide (H_2O_2), hydroxyl radical ($•O_2^-$), peroxynitrite ($ONOO^-$), aldehydes, etc., to name the most important [2–5,60]. It can be concluded that $^1O_2$ is very reactive to compounds showing double bonds, on which the oxygenation can readily proceed. And double bonds are quite abundant in organic compounds and biomolecules.

It is not my intention to review $^1O_2$ chemistry (this topic has been under study for many decades with some important contributions cited here), but just to provide a glimpse of what can happen in a biological system, like a cell, when $^1O_2$ is produced inside it or nearby. But, before briefly describing some of the most important chemical consequences of $^1O_2$ production in living systems, I would like to call the reader´s attention on a phenomenon that most probably has a large impact in the biological action of $^1O_2$: ROS interconversion. By this process one particular class of ROS reacts chemically and transforms into other ROS, which themselves can further transform into other ROS [2,17,49,60]. For example, the superoxide radical ($•O_2^-$) readily oxidizes organic compounds and gets itself reduced to H_2O_2, which further reacts to produce hydroxyl radicals (•OH), hypochlorite (OCl^-) or nitrogen dioxide ($•NO_2$). Many other reactions are possible. This testifies on the large chemical variability a researcher must face when dealing with redox biology. In fact, it is this chemical interconversion which allows part of the flexibility necessary for efficient ROS-mediated signaling [2–4].

In regards to $^1O_2$ and ROS interconversion, it is known that $^1O_2$ can produce H_2O_2 when it oxidizes certain biomolecules like ascorbate [61]. This is a critical step to explain physiological signaling mediated by $^1O_2$, as H_2O_2 is currently recognized as the main physiological signaling ROS [2–5,18–20]. A conversion from $^1O_2$ to H_2O_2 makes it more accessible to canonical redox receptors (that have evolved to recognize H_2O_2 as a signal molecule) [18], and increases the sphere of biological activity of the former $^1O_2$, as H_2O_2 has a much larger diffusion range [48]. Superoxide can be obtained directly from $^1O_2$ by one-electron reduction [62]. Peters and Rodgers reported the single-electron reaction between $^1O_2$ and different variants of NADH compounds [63]. Therefore, $^1O_2$ can engage in one-electron oxidation with the main cell reducing equivalent to convert into other ROS forms. A

conversion from $^1O_2$ to superoxide was also reported due to thermal endoperoxide activation and subsequent $^1O_2$ reaction with N,N-dimethylaniline [64]. These are proof that $^1O_2$ can be efficiently converted to other ROS, currently accepted as signaling molecules in cell biology [3,5,18,20]. Closing the circle, superoxide can promote the production of $^1O_2$ under the right conditions, like reacting with glutathione (GSH), the principal redox potential managing compound in cells [65]. This ROS interconversion is most likely a very important parameter to take into account when $^1O_2$ is generated directly by optical means. I will elaborate further on this in relation to redox biology studies at the end discussion.

3.2. Redox cell stress in relation to $^1O_2$

Following the same general historical trend of research on other ROS, the study of the biological action of $^1O_2$ dealt first with its deleterious and damaging effects on biomolecules and cells. Given its strong oxidizing nature, the production of $^1O_2$ in living systems, even in low amounts, leads to biomolecule oxidation with concomitant alteration of functional moieties/groups and loss of cellular functions [66–68]. Thus, $^1O_2$ can be considered a source of redox stress for the cell. One of the most important applications of $^1O_2$, the clinical modality known as PDT, takes advantage of the differential redox stress produced by a photodynamic treatment between tumoral and normal tissue [69]. But $^1O_2$ can be a health problem in certain circumstances, like atmospheric pollution scenarios, where sun-driven photochemistry can lead to accumulation of this and other reactive chemicals (e.g. O_3 or NOx).

Cell redox stress related to $^1O_2$ exposure has been implicated in mitotic arrest [70], cell senescence [71], inflammatory response [13,15,72], genetic damage [73–75], autophagic death [68,76], apoptosis [13,15,68], and necrosis [15,68]. In consequence, the study of biological responses to damaging concentrations of $^1O_2$ is a vigorous research area, both to protect normal cells from its effect, and to optimize PDT outcomes. Also the determination of when the damage threshold for $^1O_2$ is reached in a given system is an important question, from a basic science and health care point of view.

As mentioned before, living systems abound in biomolecules displaying double bonds and, in general, having a reductive character. The deleterious biological consequences just mentioned are a consequence of the disturbance of this reductive environment by $^1O_2$ and other ROS. In the first place, $^1O_2$ has been reported to oxidize a number of small biomolecules, cofactors and intermediate metabolites [61,63,65,68,77]. These oxidative events disrupt the signaling networks on which cell processes sit upon. For example, the increase in intracellular oxidation events leads to a change in the GSH:GSSG (glutathione disulfide) ratio, towards a less negative redox potential (i.e. to a more oxidized baseline) [20]. This, by itself, can start a stress response in the cell due to the redox signaling network based on the GSH:GSSG equilibrium [78].

Oxidative modifications of proteins by $^1O_2$ are one of the most studied areas in the biological action of $^1O_2$. The modifications with the highest biological impact are those affecting aminoacid side groups. This is because side groups provide the enzymatic capabilities of a given protein. The side groups most easily oxidized by $^1O_2$ are: cysteine, methionine, phenylalanine, tyrosine, histidine and tryptophan [16,77]. Thus, sulfur-containing or aromatic aminoacids have the largest reactivity towards $^1O_2$. The consequences of oxidative damage to proteins are diverse, but always produce a lesser or greater kind of functional disruption and loss of biological action. These can range from reversible oxidation of enzymatic or regulatory sites, to irreversible chemical changes or even peptide/protein denaturation, which can compromise essential cellular structures and processes, such as the plasmatic membrane, organelles, intracellular transit, vesicles, cell movement, mitosis, etc [66,77,79]. Additionally, oxidized proteins can act as secondary sources of ROS and increase the damaging action of these species [71,79].

Nucleic acids have been, along with proteins, the most studied area of biological impact of $^1O_2$. This can easily be understood as DNA is the reservoir of genetic information of the cell, and any chemical modification of it, such as those brought about by $^1O_2$, can lead to mutations or inadequate expression patterns. Among the elements making up DNA guanine is by far the most susceptible to oxidative damage by $^1O_2$ [74,80]. The product of guanine oxidation is the modified base 8-oxo-7,8-dihydro-2′-deoxyguanosine (8-oxo-dG). This base modification can induce mutations and, as recently reported, also epigenetic changes, if not properly excised and repaired. The mutations are mainly a consequence of G:C → T:A transversions (although other mutations are observed in minor amounts) [81]. Additionally, 8-oxo-dG can affect histone methylation patterns [82]. So, $^1O_2$ genetic impact goes further than direct mutation induction, and seems to have also an epigenetic deregulation role.

On a less subtle way, $^1O_2$ has been pointed as a direct causal agent of cytogenetic alterations [70,75]. In this case oxidative damage, both to nucleic acids and proteins, is at the root of the observed chromatin damage. On the one hand, oxidative damage to DNA is detected which signals for a rescue response. On the other hand, damage to proteins can delay this stress response, initiate its own stress response and make oxidized proteins to interact with nucleic acids in an incorrect way. This $^1O_2$-mediated cytogenetic damage is observed, not only in the cell nucleus, but also in the mitochondria, where it has been proposed as one of the main causes of age-related oxidative modifications in this organelle [73].

Currently, oxidative damage to lipids due to $^1O_2$ exposure is a very active research area. Biological lipids commonly display one or more double bonds, which make them idoneous chemical targets for $^1O_2$ oxidative action [83]. After a first reaction involving the establishment of an endoperoxide, the labile intermediate rearranges to produce lipid hydroperoxides, aldehydes and radicals [84]. These reaction products display higher hydrophilicity that the original lipids, which change the membrane properties and can critically compromise its barrier function. In addition, partially oxidized lipidic compounds can participate in further rounds of oxidative chemical reactions, with the participation of ground state $^3O_2$ [85]. These chain reaction-like oxidative waves may induce severe damage in biological membranes, compromising cell viability, and generate some amphiphilic oxidation products (e.g. aldehydes like 4-hydroxynonenal or malondialdehyde) [53,86], which can induce damage in other cellular structures (nucleus [87] or mitochondria [88], for example), and even adversely affect nearby cells (*so*-called bystander effect) [89]. Cholesterol and related compounds do react with $^1O_2$, and can start long-range damage/signaling depending on the circumstances [83,84,90].

3.3. Redox cell signaling induced by $^1O_2$

In recent years, interest in the plausible signaling role of ROS as physiological compounds has emerged as a new paradigm in biology: redox biology. $^1O_2$ is studied as one of the ROS involved in this cellular signaling. The study of the signaling roles of $^1O_2$ goes back at least 20 years, when its involvement in stress responses was acknowledged [58,91–93]. The oxidative action of $^1O_2$ exposure, if not too strong, would lead to activation of stress/rescue response in cells and tissues, mostly mediated by the stress-related JNK and p38 mitogen-activated protein kinases (MAPKs), as well as NF-κB and AP-1/AP-2 [16,72,94,95]. The final outcome depends on many parameters, but can range from cell adaptation, phenotypic changes, inflammatory response, senescence, autophagy or apoptosis.

However, as more studies are done on this topic, it is becoming clear that some ROS are able to subtly interfere with signaling networks in a positive way, i.e. to induce or enhance such processes as cell migration, cell proliferation, tissue regeneration, etc [5]. To do so, ROS must be generated in low doses, at particular cell localizations and for short

intervals [18]. *A priori*, there is no definitive reason why $^1O_2$, or its secondary ROS products, should not behave in a similar, stimulating way. In fact, several recent reports point in this precise direction [21,33,72,83,96]. The mechanisms underlying this stimulating effect are far from clear. But lessons have been learnt from other ROS, and it seems that critical cysteine residues are one of the target sensors/effectors to explain the observed results. Cell phosphatases and Src-kinases are two examples of redox regulation of cysteines. Phosphatase active sites usually have a cysteine with a catalytic role in the phosphate elimination. By oxidizing this cysteine, the catalytic activity is disrupted. A subtle oxidation (to a sulfenic state) is reversible through GSH-related activity. But stronger oxidation (sulfinic or sulfonic states) is irreversible, permanently deactivating the phosphatase. For Src-kinases the cysteines are not essential for kinase activity, but their subtle oxidation increases the enzyme activity by inducing a structural change driven by a disulfide bridge. It is known that ROS, and $^1O_2$, are able to oxidize cysteines in phosphatases [2,3,16,67,77] and Src-kinases [41,97]. So, these mechanisms can explain, at least initially, some of the stimulating effects of $^1O_2$.

In any case, researchers are just starting to tread this road, and further experimental work will be necessary in the upcoming years. It is in this area that direct optical excitation of oxygen can provide very interesting results, as will be discussed in the last section of this review. So, after these introductory sections on relevant chemical and biological aspects of $^1O_2$, we now proceed to present the photonic mechanism and available wavelengths at which $^3O_2$ can be directly pumped to $^1O_2$.

4. Direct optical excitation of $^1O_2$

It is feasible to directly excite ground state oxygen $^3O_2$ to $^1O_2$ through absorption of light energy or photons of certain energy. Although there are several procedures to excite ground state $^3O_2$ to the excited state $^1O_2$, (see Section 2.2 above), direct photonic excitation is simpler: it only requires the adequate light source. In this section, I will introduce the physical mechanism behind the photonic excitation of $^1O_2$, and the different wavelengths at which such a transition is possible. Advantages and drawbacks of each wavelength range will be discussed to offer the reader arguments to choose the best suited wavelength, depending on his or her study subject.

4.1. Optical excitation of $^1O_2$

From the beginning it must be stressed that $^3O_2$ does not strongly absorb light. At least, not in the wavelength range useful for research in redox biology. This might sound as a rotund spoiler of whatever will come next. However, the fact that oxygen does not absorb strongly does not mean that it does not absorb at all. It does, and its low absorption can be compensated by other means (light intensity, exposure time, "friendly-environment", etc.). Then, why does $^3O_2$ absorb light so weakly, and what wavelengths can we expect it to absorb?

First, molecular oxygen is a highly symmetric molecule. It is composed of two oxygen atoms which have the same electronegativity. In consequence, the molecule has no permanent dipole and for this reason $^3O_2$ does not absorb in the infrared (IR) [98]. Second, due to its exotic outer electrons arrangement (see Section 2.1), several quantum mechanical rules forbid electronic transitions between the ground state ($^3O_2$) and the two first excited states ($^1O_2$ and $^1O_2$ (b)) (see ref [8–10]. for theoretical arguments supporting these statements). Fortunately, this forbiddenness must be understood as a very low probability of such an event happening. Even more fortunate, oxygen interactions with other atoms or molecules partly relieve the molecular symmetry and change the electronic molecular orbitals, lifting to some extent the forbiddenness of these transitions. Experimental results show that $^3O_2$ can be excited efficiently enough as to observe many different responses in biological systems.

Ground state $^3O_2$ displays several absorption bands in the IR and the visible that can produce $^1O_2$ and $^1O_2$ (b) (Fig. 4) [9,22,99–104]. The particular absorption wavelengths that connect the different electronic-vibrational (vibronic) molecular levels are shown in Fig. 4B-C. Photon absorption in one of these bands leads to excitation of the corresponding singlet oxygen state, either $^1O_2$ or $^1O_2$ (b). The initial excited state can be vibrationally excited in addition (e.g. absorption at ~1065 nm produces $^1O_2$ in the first excited vibrational level or $^1O_2$ v = 1). In condensed media, like biological systems, this vibrational energy is quickly (~ps) dumped into the environment, and is of no further concern. It is worth reminding here that, whenever any optical transition favors $^1O_2$ (b) generation, this species is converted to $^1O_2$ very fast (Section 2.1), without having time to react. The absorption bands displayed in Fig. 4B are known as "monomol transitions" [9,103]. This is because the absorption of a single photon produces a single oxygen molecule in an excited state. Thus, there is a one-to-one relationship, and one mole of photons (often designed as an Einstein) will produce one mole of $^1O_2$ molecules. This nomenclature is not the most intuitive, but it is the established one, and researchers will find it over and over again in the pertaining literature.

A fascinating property of oxygen is that two transiently interacting ground state molecules [$^3O_2$–$^3O_2$] can absorb a single photon, and simultaneously reach excited electronic levels if enough energy is available [9,104]. Each molecule perturbs the other electronic orbitals when in close distance, which enhances transition probabilities. Following the nomenclature introduced in the previous paragraph, these transitions are known as "dimol transitions", as two excited molecules result after absorption of just one photon. Some observed dimol transitions are shown in Fig. 4C. In this review, I am exclusively focusing on photon absorption by molecular oxygen. But it is necessary to remark that there is reciprocity between some absorption bands and the corresponding emission bands. In other words, there is an emission band centered ~1270 nm that corresponds to the radiative deactivation of $^1O_2$ v = 0 to $^3O_2$ v = 0. Or emission at ~760 nm corresponding to $^1O_2$ (b) v = 0 to $^3O_2$ v = 0. Some practical comments concerning these emissions will be presented in Section 5.4.

In the next subsections, I will introduce monomol transitions and then dimol transitions. As a quick reference for the reader, the wavelengths, corresponding photon energies, type (monomol or dimol), and electronic states involved in each transition are summarized in Table 1.

4.2. Monomol transitions

Monomol transitions (Fig. 4B) represent the simplest excitation mechanism: a single $^3O_2$ molecule absorbs one photon and gets electronically excited, either to $^1O_2$ or $^1O_2$ (b) states. If it is the case that $^1O_2$ (b) is the generated species, it undergoes very fast conversion to $^1O_2$ (as mentioned in Section 2 [37]), which is the biologically relevant molecule. Monomol absorption bands are very weak: the corresponding molar absorption coefficients are $\sim 10^{-3}$ – $10^{-4}\,M^{-1}\,cm^{-1}$ [45,46,105–107] or even lower. These absolute values are 10^7 – 10^9 smaller than typical absorption coefficients for PDT PSs (but notice that PSs are commonly employed at 10^{-5} – 10^{-6} M final concentration). However, it is perfectly possible, as experiments show, to compensate the smaller absorption with a higher light flux and/or longer irradiation time.

The principal monomol bands are at 1270 nm, 1065 nm, 920 nm, 760 nm, 690 nm, and 627 nm. These bands will now be introduced in order of increasing photon energy (i.e. decreasing wavelength). Relevant biological reports employing these monomol transitions, along with experimental conditions and references, are listed in Table 2 as a quick guide for the interested reader.

4.2.1. 1270 nm band

This transition has an energy gap of 0.97 eV (Fig. 4B). It pumps a ground state oxygen molecule into the first excited singlet state, with no

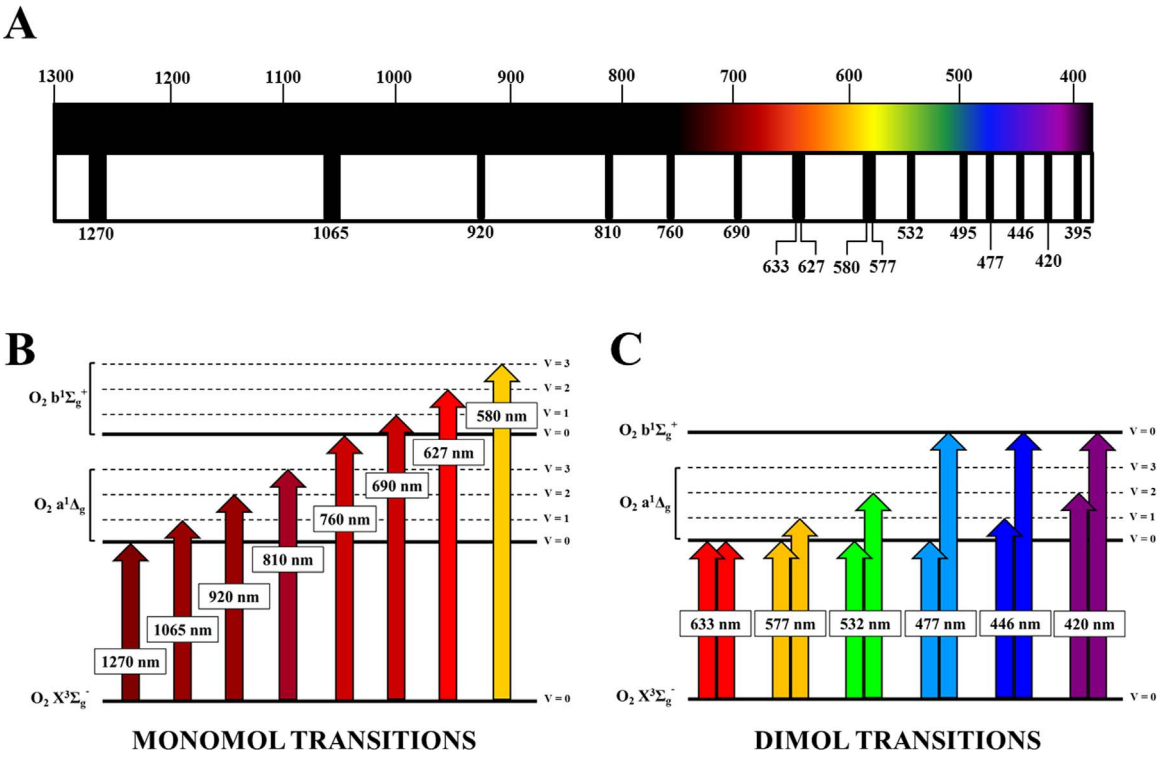

Fig. 4. Oxygen absorption bands and electronic transitions in the optical range (visible-infrared). (A) The O_2 absorption bands (black stripes) between 1300 nm and 390 nm are displayed in the spectral range covering the near-infrared and visible. The number under each transition indicates the peak wavelength, and the stripe width roughly represents the bandwidth for each transition. Both monomol and dimol transitions are plotted. All numbers refer to nanometers. (B) Monomol O_2 transitions represented in a Jablonski diagram. The peak wavelength for each transition is indicated. The arrows connect the initial level (fundamental) and the final levels, along with vibrational excitation (V > 0) in case this occurs. (C) Dimol O_2 transitions (Jablonski diagram), where two $^1O_2$ molecules are produced (double arrows) after single photon absorption. The peak wavelength for each transition is indicated. Some dimol transitions shown in (A) have not been represented here. Data based on [35,99–104,107].

additional vibrational energy ($^3O_2$ v = 0 → $^1O_2$ v = 0). The band is relatively broad (± 20 nm), although the final width depends on the particular solvent in which O_2 is dissolved [105–107]. However, given the very low absorption coefficient and the band narrowness, it is advisable to try to use light sources with emission as close to the band peak as possible (see Section 5.3). This is even more advisable for all the O_2 bands to be subsequently discussed. The excitation of $^1O_2$ using 1270 nm was already introduced in the late 1960s and early 1970s, to obtain $^1O_2$ in gas-phase oxygen at very high pressures (tens or hundreds of bars) or in different organic solvents for physical chemical studies [36,99,100]. These conditions were selected to make up for the low absorption at this wavelength. In these experiments oxygenation of chemical traps was demonstrated by directly exciting $^1O_2$ optically. However, light sources emitting around 1270 nm were scarce, mainly due to lack of practical applications for this wavelength range. In consequence, experiments employing light around 1065 nm were much more common because of the coincidence of this band with the light emitted by neodymium lasers (see 1065 nm band below).

It was not until the late 1980s that this band was given proper attention, this time for biological and clinical applications [108]. Former Soviet Union researchers and clinicians employed this and other bands in what has been called the “light-oxygen effect” or LOE. In their 1999 review on this topic, Zakharov and Ivanov present a series of experimental results comparing efficiency of LOE vs. classical PDT as to biological outcomes. To study biological effects at 1270 nm they employed an InGaAsP/InP semiconductor laser. They assessed the light effect on erythrocytes suspensions by changes in the refractive index and alterations of the cell membrane. Introducing N_2 in the system abrogated the changes and the cell response followed the IR absorption band of $^3O_2$. The authors also report the use of continuous wave (cw) lasers tuned at 1264 ± 9 nm to treat tumors in mice in 1993. In these experiments the animals were exposed to light powers of 8.5 mW for times of 10 min (several days).

Then, in 2003 Krasnovsky *et al.* reported on the photonic production of $^1O_2$ under experimental conditions “using laser generators approximately that power which was used in biological experiments” [109]. They employed a cw diode laser (1266 ± 4 nm P = 55 mW) and a pulsed tunable forsterite laser (tuning range 1200–1290 nm P = 30–150 mW-average) to produce $^1O_2$ to be trapped by aromatic compounds. The interesting aspect is that the authors measured $^1O_2$ production by light in several atmospheric pressure air-saturated solvents at room temperature, including H_2O. Their results pointed indeed to $^1O_2$ production to explain the observed chemical trap bleaching. And positive results were obtained in H_2O, even when it is, probably, the most unfavorable solvent to achieve efficient $^1O_2$ production. Following this, in a series of publications, Krasnovsky *et al.* further substantiated the real possibility to achieve $^1O_2$ generation by direct optical pumping in relevant amounts for chemical or biological studies [110–114]. The action spectrum for $^1O_2$ production fitted precisely with the IR absorption band peaking at 1270 nm. The efficiency of the process was higher in organic solvents than in D_2O. The presence of $^1O_2$-quenchers, like sodium azide (NaN_3) or β–carotene, effectively decreased $^1O_2$ excitation, as did purging with N_2. Of special relevance in this sense is a work published in 2008 in which $^1O_2$ was generated by a cw semiconductor laser emitting at 1269 nm with a maximum power of 700 mW in H_2O-SDS micellar systems [114]. Chemical trap photooxygenation was observed under laser irradiation in air-saturated aqueous solutions (some preliminary work was done in H_2O-micelles in 2006 [112]). Therefore, $^1O_2$ photonic generation was shown to be feasible under conditions very close to those of biological relevance.

From 2010 onwards, reports on the direct optical excitation of $^1O_2$

Table 1
Molecular oxygen optical transitions between the ground state (O_2 $X^3\Sigma_g^-$) and the first two electronic excited states (O_2 $a^1\Delta_g$) and (O_2 $b^1\Sigma_g^+$). The transitions are listed in order of increasing energy (eV) (decreasing wavelength in nm). Both monomol (M) and dimol (D) transitions are shown. Data based on [35,99–104,107].

Wavelength	Photon energy	Type (M-Monomol; D-Dimol)	Electronic transition
1270 nm	0.97 eV	M	O_2 $X^3\Sigma_g^-$ → O_2 $a^1\Delta_g$ v = 0
1065 nm	1.16 eV	M	O_2 $X^3\Sigma_g^-$ → O_2 $a^1\Delta_g$ v = 1
920 nm	1.35 eV	M	O_2 $X^3\Sigma_g^-$ → O_2 $a^1\Delta_g$ v = 2
810 nm	1.53 eV	M	O_2 $X^3\Sigma_g^-$ → O_2 $a^1\Delta_g$ v = 3
760 nm	1.63 eV	M	O_2 $X^3\Sigma_g^-$ → O_2 $b^1\Sigma_g^+$ v = 0
690 nm	1.80 eV	M	O_2 $X^3\Sigma_g^-$ → O_2 $b^1\Sigma_g^+$ v = 1
633 nm	1.96 eV	D	[O_2 $X^3\Sigma_g^-$ - O_2 $X^3\Sigma_g^-$] → [O_2 $a^1\Delta_g$ v = 0 - O_2 $a^1\Delta_g$ v = 0]
627 nm[a]	1.98 eV	M	O_2 $X^3\Sigma_g^-$ → O_2 $b^1\Sigma_g^+$ v = 2
580 nm[a]	2.14 eV	M	O_2 $X^3\Sigma_g^-$ → O_2 $b^1\Sigma_g^+$ v = 3
577 nm	2.15 eV	D	[O_2 $X^3\Sigma_g^-$ - O_2 $X^3\Sigma_g^-$] → [O_2 $a^1\Delta_g$ v = 1 - O_2 $a^1\Delta_g$ v = 0]
532 nm[a]	2.33 eV	D	[O_2 $X^3\Sigma_g^-$ - O_2 $X^3\Sigma_g^-$] → [O_2 $a^1\Delta_g$ v = 2 - O_2 $a^1\Delta_g$ v = 0]
495 nm[a]	2.50 eV	D	[O_2 $X^3\Sigma_g^-$ - O_2 $X^3\Sigma_g^-$] → [O_2 $a^1\Delta_g$ v = 3 - O_2 $a^1\Delta_g$ v = 0]
477 nm[a]	2.60 eV	D	[O_2 $X^3\Sigma_g^-$ - O_2 $X^3\Sigma_g^-$] → [O_2 $a^1\Delta_g$ v = 0 - O_2 $b^1\Sigma_g^+$ v = 0]
446 nm[a]	2.78 eV	D	[O_2 $X^3\Sigma_g^-$ - O_2 $X^3\Sigma_g^-$] → [O_2 $a^1\Delta_g$ v = 1 - O_2 $b^1\Sigma_g^+$ v = 0]
420 nm[a]	2.95 eV	D	[O_2 $X^3\Sigma_g^-$ - O_2 $X^3\Sigma_g^-$] → [O_2 $a^1\Delta_g$ v = 2 - O_2 $b^1\Sigma_g^+$ v = 0]
395 nm[a]	3.14 eV	D	[O_2 $X^3\Sigma_g^-$ - O_2 $X^3\Sigma_g^-$] → [O_2 $a^1\Delta_g$ v = 3 - O_2 $b^1\Sigma_g^+$ v = 0]
380 nm[a]	3.26 eV	D	[O_2 $X^3\Sigma_g^-$ - O_2 $X^3\Sigma_g^-$] → [O_2 $b^1\Sigma_g^+$ v = 0 - O_2 $b^1\Sigma_g^+$ v = 0]
360 nm[a]	3.44 eV	D	[O_2 $X^3\Sigma_g^-$ - O_2 $X^3\Sigma_g^-$] → [O_2 $b^1\Sigma_g^+$ v = 1 - O_2 $b^1\Sigma_g^+$ v = 0]
344 nm[a]	3.60 eV	D	[O_2 $X^3\Sigma_g^-$ - O_2 $X^3\Sigma_g^-$] → [O_2 $b^1\Sigma_g^+$ v = 2 - O_2 $b^1\Sigma_g^+$ v = 0]

[a] Transitions included for completeness but not discussed in depth in the text.

at 1270 nm for biomedical goals have experienced a large increase. In 2010 a Raman-shifted laser source (1262 nm and 5.5 W) has been employed to successfully treat tumoral skin lesions in human patients [23]. It should be remarked, nonetheless, that photothermal effects cannot be ruled out due to the high power of the laser (see Section 5.6). In any case, an additive or synergic effect would be welcome, if it increases the chances of a positive clinical outcome. Also in 2010 Anquez *et al.* started a series of publications on direct excitation of $^1O_2$ in the 1270 nm band under different experimental parameters. In their first contribution, $^1O_2$ was generated using a Raman fiber ring laser (1240–1289 nm 2.5 W) in ethanol and acetone air-saturated solutions [115]. The detection of $^1O_2$ was achieved through the use of a chemical trap. The action spectrum displayed a good fitting with $^3O_2$ absorption spectrum in the NIR.

Following this first approach, Anquez et al. proved that irradiation of living human and rat tumoral cells under normal conditions (air-saturated growing medium) at ~1270 nm (100 W cm^{-2} 1.5–3 h exposure) induced cell death [24,25]. Cell images seem to fit with necrotic death morphology, after plasmatic membrane integrity loss and subsequent osmotic shock. Several complementary experiments point to the involvement of $^1O_2$ as the cytotoxic agent: increase of cytotoxicity with higher pO_2, decrease after N_2 purging, action spectrum fitting $^3O_2$ NIR absorption spectrum, and decrease in toxicity in the presence of $^1O_2$-quenchers (bovine serum albumin –BSA- and NaN_3). Additionally the authors took care in regards to the plausible temperature increase during NIR laser irradiation. Their results permitted to dismiss photothermal action as the damaging agent. This group has published more experimental results on $^1O_2$ photonic excitation at 1270 nm, covering biological [116] and chemical [117,118] models.

Other research groups have also recently explored the usefulness of the 1270 nm band. The group led by Rafailov has studied and modelled the oxidative stress induced by $^1O_2$ excited at 1268 nm (cw semiconductor laser up to 500 mW) [27,119,120]. Their models support the argument that an initial $^1O_2$ burst leads to a redox imbalance, which destabilizes cell metabolism well after actinic light exposure has ended. This is a very interesting topic, with far-reaching consequences and will be further discussed in Section 5.2. Further experiments employing a 1265 nm cw excitation have been done by Kurkov *et al.*, where oxidative stress and regression was induced in experimental animal tumors [26], and oxidative mitochondrial and overall cell disruption was recently obtained in cell cultures [28]. As mentioned in relation with some of the experimental results presented, the main concern using this band is its photothermal potential due to IR water absorption [121]. Thermal aspects of direct optical excitation of $^1O_2$ will be discussed together in Section 5.6 below.

4.2.2. 1065 nm band

This band has an energy gap of 1.16 eV (Fig. 4B). It involves a transition of a ground state molecule into the first excited singlet state, with concurrent excitation of its first vibrational level ($^3O_2$ v = 0 → $^1O_2$ v = 1). The band is also relatively broad (± 15 nm), again depending on the gas pressure or the particular solvent in which O_2 is dissolved [103]. The absorption coefficient is smaller than the 1270 nm transition [99,102,103,105]. After excitation, the vibrational energy decays very fast releasing heat to the environment, so for any practical biological purpose excitation at 1065 nm is equal to excite at 1270 nm. Two are the main advantages, one fundamental and the other one practical, of using 1065 nm in biological research: the tenfold reduction in water absorption as compared to 1270 nm [121], and the coincidence of this absorption band with the emission from commercially-available neodymium-based lasers (~1064 nm).

Experiments employing this band to excite $^1O_2$ started in the 1970s, basically aiming to address several physical chemical parameters like chemical reactions and reaction rates [99,100,122–125], oxygen luminescence [101,126–128], or even oxygen lasing in the red and IR [129] (for more recent studies on molecular oxygen lasing schemes see also [130–133]). In fact, one of the first determinations of $^1O_2$ reaction rates with aminoacids was obtained by optically pumping $^1O_2$ at 1064 nm in D_2O, which thereafter reacted with histidine, tryptophan, methionine, tyrosine and alanine (in this order of decreasing reactivity) [134].

Due to their availability and reliability, Nd-based lasers have found an important niche in biological studies as light sources for optical tweezers. Optical tweezers allow the trapping and controlled movement of microscopic entities (e.g. cells) by focusing the light or making adequate interference patterns. At ~1064 nm photon absorption by biological chromophores is negligible as long as one stays in the linear excitation regime, i.e. irradiance < MW cm^{-2}. Thus, Nd lasers, mainly Nd-YAG, are widely employed as sources for optical tweezers. However, several publications have reported chemical and biological damage at relatively low light intensities in optical traps at this wavelength [30,31,135–142]. In many of these publications the source of damage has been ascribed to direct thermal action (due to water absorption), organic chromophore excitation in the limit of the absorption band (*e.g.* cell cytochromes) or biphotonic excitation. Very few articles point directly to $^1O_2$ excitation as a plausible source of damage, although some of them show cell damage action spectra that fit reasonably well with the absorption spectrum of $^3O_2$ and invoke ROS as a general disruption mechanism [136–138,142]. On the other hand, experiments by Landry et al. provide direct evidence for $^1O_2$ production in an optical tweezers setup [30]. The authors show that depleting the medium of O_2 eliminates the oxidative damage to a DNA molecule stretched between two microscopic beads trapped by the optical tweezers. Oxidative damage to DNA is linearly proportional to laser power (*i.e.* one-photon process) and addition of $^1O_2$ quenchers (*e.g.* NaN_3 and ascorbic acid)

Table 2
Relevant examples of biological experiments with monomol O_2 transitions. Several experimental aspects are detailed in each entry (see footnotes for more information). Each set of conditions has been obtained from a publication, with the particular reference provided in each case.

Transition	Biological model	Light source	Wavelength	Power	Spectral control	$^1O_2$ scavenging	$^1O_2$ enhancement	Thermal control	Reference
1270 nm	Human erythrocytes	Diode laser (cw)	1264 nm	0.5–2 mW	Yes	pN_2	No	No	[108]
	T36 carcinoma in mice	Diode laser (cw)	1264 nm	4–4.5 mW	No	No	No	No	[108]
	Human skin tumors	Raman fiber laser (cw)	1262 nm	1.5–5 W	No	No	No	No	[23]
	MCF-7 breast cancer line	Raman fiber laser (cw)	1270 nm	1.5–5 W	Yes	-BSA -NaN_3 -pN_2	pO_2	Yes	[24]
	CC-5 carcinoma in mice	Raman fiber laser (cw)	1265 nm	4 W	No	No	No	No	[26]
	-HaCaT -Primary Keratinocytes -HeLa	Diode laser (cw)	1268 nm	500 mW	Yes	α-TOC	No	Yes	[27]
	MCF-7 breast cancer line	Raman fiber laser (cw)	1270 nm	300 mW	Yes	-BSA -NaN_3 -pN_2	pO_2	Yes	[116]
	-HaCaT -Primary Keratinocytes -HeLa	Diode laser (cw)	1268 nm	–	No	No	No	No	[119]
	-HCT-116 colorectal line -CHO-K ovarian line	Raman fiber laser (cw)	1265 nm	4 W	No	No	No	Yes	[28]
1065 nm	NC-37 lymphoblast line	Nd: YAG laser (cw)	1064 nm	60–240 mW	Yes	No	No	Yes	[138]
	E. coli bacteria	Nd: YAG laser (cw)	1064 nm	3–30 mW	No	No	No	Yes	[139]
	Human skin fibroblasts	Nd: YAG laser (cw)	1064 nm	1 W	Yes	No	No	Yes	[143]
	Double strand DNA	Nd: YAG laser (cw)	1064 nm	30–350 mW	No	-O_2 depletion -Ascorbate -Lipoic acid -NaN_3	No	Yes	[30]
	S. cerevisiae yeast	Yb fiber laser (cw)	1070 nm	0.7–2.6 mW	No	No	No	Yes	[31]
920 nm	*E. coli* bacteria	Ti: sapphire laser (cw)	900 nm	5–19.1 mW	Yes	No	No	Yes	[145]
	-A549 adenocarcinoma -PtK2 renal line -U2OS osteosarcoma	LED (cw)	901 ± 69 nm	–	Yes	No	No	Yes	[146]
810 nm	NC-37 lymphoblast line	Ti: sapphire laser (cw)	800 nm	60–120 mW	Yes	No	No	Yes	[138]
	C. elegans nematode	Ti: sapphire laser (cw)	810 nm	240–480 mW	Yes	No	No	Yes	[147]
	Rat lymphoblasts	Diode laser (cw)	808 nm	30–100 mW	No	No	No	No	[149]
	Mouse primary neurons	Diode laser (cw)	810 nm	–	No	No	No	No	[154]
	C2C12 myoblast line	Diode laser (cw)	808 nm	100 mW	No	No	No	No	[151]
	Rat muscle (hind leg)	Diode laser (cw)	808 nm	100 mW	No	No	No	No	[152]
760 nm	PtK2 renal line	Ti: sapphire laser (cw)	760 nm	130 mW	Yes	No	No	Yes	[161]
	-Human sperm cells -CHO line	Ti: sapphire laser (cw)	760 nm	70–88 mW	Yes	No	No	No	[162]
	-Human sperm cells -CHO line	Ti: sapphire laser (cw)	760 nm	70–88 mW	Yes	No	No	No	[163]
	CHO line	Ti: sapphire laser (cw)	760 nm	88–176 mW	Yes	No	No	Yes	[136]

(continued on next page)

Table 2 *(continued)*

Transition	Biological model	Light source	Wavelength	Power	Spectral control	$^1O_2$ scavenging	$^1O_2$ enhancement	Thermal control	Reference
	CHO line	Ti: sapphire laser (cw)	760 nm	88–176 mW	Yes	No	No	Yes	[164]
	Human erythrocytes	Ti: sapphire laser (pulsed)	762 nm	200 mW	Yes	No	No	Yes	[108]
	Lewis carcinoma in mice	Alexandrite laser (pulsed)	762 nm	200 mW	No	No	No	No	[108]
	NC-37 lymphoblast line	Ti: sapphire laser (cw)	800 nm	60–120 mW	Yes	No	No	Yes	[138]
	C. elegans nematode	Ti: sapphire laser (cw)	760 nm	240–480 mW	Yes	No	No	Yes	[147]
	HeLa line	Ti: sapphire laser (pulsed)	765 nm	700 mW (pre-stage)	Yes	-NaN_3 -α-TOC	D_2O	Yes	[32]
	HeLa line	Ti: sapphire laser (pulsed)	765 nm	4.5–91.5 mW (on-stage)	Yes	No	No	Yes	[33]
690 nm	Human fibroblasts	Diode laser (cw)	692 nm	30 mW	Yes	No	No	No	[168]

Spectral control means that the biologically-relevant wavelength has been compared to other close wavelengths in the experiments. $^1O_2$ scavenging informs if any of the following measures have been employed to scavenge or quench $^1O_2$ activity: BSA (added Bovine Serum Albumin); pN_2 (increasing N_2 pressure in the system to displace O_2); NaN_3 (added sodium azide); α-TOC (added α-tocopherol); O_2 depletion (O_2 consumption by added enzymatic oxidases). $^1O_2$ *enhancement* alludes to strategies to increase $^1O_2$ activity: pO_2 (pumping O_2 into the system to increase its partial pressure); D_2O (added deuterium oxide). *Thermal control* means that either the researchers have taken active measures to control the setup temperature during irradiation or, at least, they accounted for a possible photothermal activity of the actinic light in the article.

greatly diminishes it too. However, the authors point to the polystyrene beads employed to tether the DNA as the source of $^1O_2$. Although not completely negating this possibility, the alternative view that $^1O_2$ is being directly excited by 1064 nm photons should be considered. As other IR wavelengths are employed in optical tweezers, and some of them overlap $^3O_2$ absorption bands, I will discuss further the oxidative damage in optical traps in Section 5.5.

Some research groups have focused on this wavelength range to directly perturb living systems. Abrahamse *et al.* have compared 1064 nm vs. 632.8 nm and 830 nm exposure of fibroblast cultures [29,143,144]. Some cell damage was observed a few days after laser exposure especially in the 1064 nm group. At high light doses the two groups displaying higher levels of damage were 632.8 nm and 1064 nm, a dimol (see below) and monomol O_2 absorption bands. The authors theorize that this damage is not of thermal origin and hint that ROS could be the source. Although this group has later focused in the biological effects of shorter wavelengths, their former results with 1064 nm light indicate that there is a significant biological activity at that wavelength. Thermal issues can be something to consider, but water absorption is one order of magnitude lower at 1065 nm in respect to 1270 nm. Therefore 1065 nm seems *a priori* a better excitation source for redox biology studies concerning $^1O_2$.

4.2.3. 920 nm band

This band corresponds to the transition ($^3O_2$ v = 0 → $^1O_2$ v = 2) with a photon energy of 1.35 eV. The transition probability decreases exponentially the higher the final vibrational level and, in consequence, this wavelength has been scarcely employed for biological studies. It displays a low absorption by water but nevertheless only half that of 1065 nm light [121], which does not compensate for the decrease in the $^3O_2$ absorption coefficient. Nowadays is easier to find light sources at ~920 nm but sources at ~1065 nm are still much more widespread.

This wavelength range is employed in optical traps where some biological side effects are reported. Liang *et al.* studied the action spectrum for cell perturbation in the range 700–1100 nm [136]. They found a marked decreased in cell clonal growth at ~900 nm (along 1064 nm and 740–760 nm). The authors dismiss a thermal mechanism of damage and suggest that biphotonic processes could explain the observed biological effect. Two articles studied the optimal NIR region for bacterial (*E. coli*) optical trapping. Neuman *et al.* observed a clear deleterious effect on bacterial movement (taken as a proxy of viability) around 915 nm [137]. The effect was dependent on oxygen presence and showed one-photon dependence. The authors directly point to $^1O_2$ as a most plausible source of damage although photosensitized by some "sensitizer molecule". They acknowledge that $^1O_2$ can be directly photoexcited but, most surprisingly, they state that "…the absorption spectrum for molecular oxygen does not resemble the action spectrum for *E. coli*.". A further paper was published in 2008 assessing again the action spectrum for bacterial photodamage between 840 and 930 nm [145]. There is a marked increase in bacterial metabolic inactivation and killing at 900 and 930 nm (more severe at this wavelength) when compared to 840 and 870 nm. The photodamage is linear with light intensity although a hypothesis involving biphotonic excitation of GFP (which was employed to label the bacteria) was advanced to try to explain the lack of putative chromophore. Oxygen is not considered and, in the end, the authors state: "A specific photochemical cause of photodamage eludes us—the spectrum is not consistent with water or *E. coli* or the media.". Additional comments of $^1O_2$ generation in optical traps will be provided in Section 5.5.

Recently Spitler and Berns have published interesting results on cell photostimulation and in vitro wound healing [146]. They employed light emitting diode (LED) arrays to increase cell proliferation and migration in several cell lines. The most successful excitation was obtained with LEDs emitting at 901 nm (peak), but with a very broad emission spectrum (full bandwidth at half maximum –FWHM- of 69 nm), fully overlapping the 920 nm oxygen band. Generation of $^1O_2$

or other ROS is not mentioned, but light absorption by elements of the mitochondrial electron transport chain (cytochrome c oxidase) is proposed as a possible chromophore to explain the results (see Section 5.3 for more on O_2 absorption vs. endogenous chromophores). Anyway, this article highlights the use of LEDs as alternative light sources to lasers for O_2 optical excitation (Section 5.3).

4.2.4. 810 nm band

This band corresponds to the transition ($^3O_2$ v = 0 → $^1O_2$ v = 3) with a photon energy of 1.53 eV. It has been widely employed in photobiological studies given the availability of diode lasers emitting at 808 nm. In addition, wavelengths between 800 and 850 nm show very low absorption in biological systems, due to the lack of endogenous chromophores absorbing in this range and the still very low water absorption in this region of the NIR (see for more on the so-called biological window). At this wavelength the transition probability is extremely small and, in fact, absorption by other chromophores, like cytochromes, should complementary be considered to explain the biological responses observed.

This wavelength range is popular in optical traps due to the very low level of damage observed in bacteria [137], eukaryotic cells [136,138] and in whole organisms (*C. elegans*) [147]. Nevertheless, the light is not innocuous. Under the right irradiation conditions cell growth inhibition has been reported. Under long irradiation times the growth and proliferation of a human glioblastoma cell line was significantly inhibited [148]. Studies led by Fonseca have found evidence of genetic damage [149], increased mRNA and protein expression involved in DNA repair and genomic stabilization [150], and increasing occurrence of both apoptosis and necrosis [151] in white blood cells and myoblasts exposed to 808 nm light. Both gross chromatin alterations (comet assay) as well as base-level oxidative modifications (8-oxo-dG) were observed. These genetic alterations, although not exclusive of $^1O_2$ action, strongly point to its production during light exposure. Quite recently this group has found concerning evidence of ploidy alterations (changes in the cell chromosomal set) and a trend in DNA fragmentation (not statistically significant) in muscles exposed to 808 nm light [152].

In contrast, Yu et al. have found a protective role of 810 nm light in an oxygen-glucose deprivation neuronal model in vitro [153,154]. However the light fluence employed (3 J cm^{-2}) with a cw diode 810 nm laser is between 3 and 23 times smaller than that employed by Fonseca *et al.* Again, this pinpoints the importance of dose in inducing stimulating or deleterious biological effects.

4.2.5. 760 nm band

This band presents the peculiarity that the produced singlet oxygen species is the second excited state ($^3O_2$ v = 0 → $^1O_2$ (b) v = 0) [35–37]. The transition energy is 1.63 eV and the bandwidth is fairly narrow (± 10 nm) [9,46,113]. In aqueous solutions its decay lifetime is very short, on the order of picoseconds, and it can be assumed that all $^1O_2$ (b) produced is converted to $^1O_2$ with unity efficiency [37]. The direct optical excitation of $^1O_2$ (b) has been successfully employed both in past decades, and recently in the field of physical chemistry [6,7,99,100,102,155–160].

Research done mainly in the last decade has shown that it is feasible to directly excite $^1O_2$ (b) at ~760 nm in different solvents [46,106,110], but particularly in H_2O, D_2O and aqueous solutions [32,46,105,107]. In consequence, given H_2O role as universal solvent in biological systems, the production and biological activity of $^1O_2$ (b) after exposure to 760–765 nm light was proposed and demonstrated recently [32–34]. Experiments were done with a pulsed Ti:sapphire laser with different average powers and irradiation times (5–100 mW and 10 s – 10 min) focused inside HeLa cells. As a result, different cell responses have been produced, which ranged from fast necrosis to cell proliferation stimulation [33]. Additionally, irradiations were done just outside cells and necrosis was also achieved, an important issue in the study of the sphere of action of $^1O_2$ (b). The primary role of $^1O_2$ in the biological responses was demonstrated by an enhanced effect in solutions partly prepared with D_2O, the inhibitory action of $^1O_2$-quenchers (NaN_3 and α-tocopherol), the negligible effect of catalase (H_2O_2 quencher), and the establishment of a biological action spectrum for cell death, in almost perfect coincidence with $^3O_2$ absorption between 730 and 800 nm. Additional evidence was obtained when a cw Ti:sapphire laser induced necrosis in single cells at 763 nm, but not at 800 nm, thereby ruling out any non-linear optical process (Blázquez-Castro, Haro and Jaque, unpublished results).

But the biological action of light in the 750–770 nm range has been observed much earlier, although in practically all the cases it went unrecognized as the consequence of the direct optical excitation of oxygen. In the early 1990s optical trapping was rapidly developing as a biological manipulation technique. Researchers were interested in finding the safer wavelength range to study samples. So efforts to establish an action spectrum of biological damage (expressed in different ways, from loss of mobility to outright cell killing) were done (some results concerning this have already been presented in previous O_2 bands). Several publications came to the conclusion that the region around 765 nm should be avoided. Deleterious biological effects observed to support this argument include positive genetic comet assay [138], heat shock response in *C. elegans* [147], chromosomal damage [161], loss of spermatozoa mobility [162], loss of cell cloning efficiency [136,162,163], propidium iodide internalization [163], and giant cell/coenocyte formation [164]. Most publications point to some biphotonic effect as the cause of these negative responses, some also mentioning the possibility that ROS (in general) could be involved. Somewhat surprisingly König et al. found no differential biological effect in cell cloning efficiency when cells were exposed to 760 nm vs. 730 and 800 nm [165]. A possible explanation for this result can be that the irradiances employed in the experiments were relatively high (10^{12} W cm^{-2}) which, as pointed by the authors, can lead to plasma generation inside the cell. Damage due to plasma formation would surpass any effect $^1O_2$ production could induce.

The recent biological results obtained at ~760 nm, both damaging [32] and stimulating [33], seem to contradict the very low $^3O_2$ absorptivity and small $^1O_2$ amount generation. It can happen, however, that cells are more susceptible to $^1O_2$ than suspected earlier. I will discuss this in Section 5.2. Additionally, as timely pointed out recently by Krasnovsky and Kozlov, the absorption coefficients of $^3O_2$ at 1273 nm and 765 nm in aqueous solutions are practically equal [107]. More arguments in favor of employing one or the other wavelength band in redox biology research will be provided in Section 5.3. Some preliminary research in tumor regression was done in the early 1990s with a pulsed alexandrite laser emitting at 762 nm [108]. The researchers observed a significant tumor growth suppression and average lifespan extension of 50% in the treated mice.

4.2.6. 690 nm band

Absorption in this band promotes the following transition ($^3O_2$ v = 0 → $^1O_2$ (b) v = 1). The energy gap is 1.80 eV, in the far red optical spectrum. Few publications cite results dealing with this band, which mainly involve spectroscopy and $^1O_2$ quenching studies [157,158,166,167]. The transition probability is quite small, and it overlaps greatly with endogenous chromophores present in living cells. Some biological results were published by Almeida-Lopes *et al.* after laser diode exposure (one of them emitting at 682 nm) of human gingival fibroblasts in vitro [168]. Growth curves point to a subtle stimulating effect of 692 nm over controls and cultures exposed to 786 nm during the first 4 days. The effect disappears by day 6 post treatment. Precisely due to this band overlap with endogenous chromophores its use in redox biology studies is discouraged, as it is more difficult to reach valid conclusions on the working mechanisms, both chemical and biological.

4.3. Dimol transitions

These transitions excite two singlet oxygen molecules while just one photon (hν) is absorbed by the momentary complex formed by two ground state molecules: [$^3O_2$ - $^3O_2$] + hν → [$^1O_2$ - $^1O_2$] [104]. The singlet oxygens produced can be vibrationally excited or not, or one can be in the first excited state ($^1O_2$) and the other in the second excited state ($^1O_2$ (b)). The dimol transitions are listed in Table 1 and displayed in Fig. 4C. As these transitions depend on the temporal establishment of the [$^3O_2$ - $^3O_2$] collision pair, the absorption coefficient depends on the square of the oxygen partial pressure (pO_2). The pO_2 in air-saturated aqueous solutions is around 0.27 mM, thus it follows that dimol bands are relatively weak in comparison to the monomol transitions introduced previously. This is an important argument discouraging their use in redox biology in favor of monomol excitations. Another argument is that dimol transitions cover a range of wavelengths between 633 nm in the visible and 344 nm in the UV (see Table 1). These wavelengths overlap the absorption bands of numerous endogenous chromophores, from cytochromes in the far visible [169,170] to cofactors and aminoacids in the UV [171,172]. Therefore it becomes very difficult to discern which chromophores and ROS get involved in a particular biological response after light exposure at these wavelengths. Nevertheless some of them are very popular, in particular light of 633 nm, in the so-called low-level laser therapy (LLLT), and I will introduce briefly the main dimol transitions. Relevant biological works employing dimol transitions are listed in Table 3.

4.3.1. 633 nm band

Absorption of one 633 nm photon promotes the following dual transition: [$^3O_2$ - $^3O_2$] + hν → [$^1O_2$ v = 0 - $^1O_2$ v = 0]. Basically it is the dimol counterpart of the 1270 nm monomol transition (two 1270 nm photons have the same energy as one 633 nm photon), with an energy of 1.96 eV. This transition has been employed to assess physical and/or chemical parameters, mainly in high pressure oxygen although there are studies in organic solvents too [99,101,123,173–176].

Its popularity in biological studies comes from the fact that the band coincides with the emission of the very common Helium-Neon (He-Ne) laser at 632.8 nm. Thus, He-Ne laser availability has made studies at this wavelength quite accessible. There are literally hundreds of scientific publications on the biological action of He-Ne laser. Most of them study the photomodulation and photostimulation of cells, tissues and animals within the frame of LLLT [108,141,143,177–180] although some studies also report on the damaging action when high light doses are employed [29,181]. LLLT is currently a very active and broad research and clinical area. It is therefore outside the scope of this review which tries to focus explicitly in the direct excitation of $^1O_2$. The interested reader can consult some of the cited references for more specific sources and information on this very appealing topic (see also the review by Chung *et al.* for an interesting introduction to LLLT [182]).

It is worth mentioning that, by pure chance, the 633 nm dimol transition overlaps with a 627 nm monomol transition. This monomol band corresponds to the initial excitation of $^1O_2$ (b) v = 2 [157,158,167]. However its absorption coefficient is very low. But it seems interesting, in regards to the mechanistic action of LLLT, to keep in mind that exciting at ~633 nm can in fact excite $^1O_2$ by two complementary transitions: a monomol and a dimol.

4.3.2. 577 nm band

Absorption of a ~577 nm photon leads to the following transition [$^3O_2$ - $^3O_2$] + hν → [$^1O_2$ v = 1 - $^1O_2$ v = 0]. One of the $^1O_2$ molecules is produced in the first vibrational state which rapidly deactivates to the v = 0 level releasing heat [174,183]. This wavelength range is routinely employed in the photothermal treatment of vascular disorders making use of pulsed dye lasers [184]. The possibility that a partial effect is due to $^1O_2$ excitation cannot be ruled out, but evidence points

Table 3
Relevant examples of biological experiments with dimol O_2 transitions. Several experimental aspects are detailed in each entry (see footnotes for more information). Each set of conditions has been obtained from a publication, with the particular reference provided in each case.

Transition	Biological model	Light source	Wavelength	Power	Spectral control	$^1O_2$ scavenging	$^1O_2$ enhancement	Thermal control	Reference
633 nm	Human erythrocytes	Dye laser (pulsed)	633 nm	–	Yes	No	No	No	[108]
	Human erythrocytes	He-Ne laser (cw)	632.8 nm	38–50 mW	No	pAr	pO_2	Yes	[108]
	NC-37 lymphoblast line	He-Ne laser (cw)	633 nm	1.2 mW	No	No	No	No	[177]
	A2058 melanoma line	He-Ne laser (cw)	632.8 nm	7 mW	No	No	No	Yes	[178]
	Human skin fibroblasts	He-Ne laser (cw)	632.8 nm	18.8 mW	Yes	No	No	Yes	[143]
	MCF-7 breast cancer line	He-Ne laser (cw)	632.8 nm	14 mW	No	No	No	No	[141]
	-A549 -EMT6 -ASTC-a-1	Diode laser (cw)	635 nm	–	No	-SOD -NAC	No	No	[181]
	-EMT6 tumors in mice -ASTC-a-1 tumors in mice	Diode laser (cw)	635 nm	–	No	No	No	No	[181]
	-A549 adenocarcinoma -PtK2 renal line -U2OS osteosarcoma	LED (cw)	637 ± 17 nm	–	Yes	No	No	Yes	[146]
	Clinical trials in women	Diode laser (cw)	635 nm	–	No	No	No	No	[180]
577 nm	Human erythrocytes	Dye laser (pulsed)	585 nm	70–300 mW	Yes	No	No	Yes	[108]

Spectral control means that the biologically-relevant wavelength has been compared to other close wavelengths in the experiments. *$^1O_2$ scavenging* informs if any of the following measures have been employed to scavenge or quench $^1O_2$ activity: pAr (increasing Argon pressure in the system to displace O_2); SOD (added Superoxide Dismutase); NAC (added N-acetyl cysteine). *$^1O_2$ enhancement* alludes to strategies to increase $^1O_2$ activity: pO_2 (pumping O_2 into the system to increase its partial pressure). *Thermal control* means that either the researchers have taken active measures to control the setup temperature during irradiation or, at least, they accounted for a possible photothermal activity of the actinic light in the article.

to a purely thermal mechanism of action. However there is at least one example in which a biological response has been measured and assigned to direct $^1O_2$ excitation at ~577 nm. Armichev *et al.* reported on changes in the plasmatic membrane permeability of red blood cells exposed to a tunable dye laser emitting between 570 and 590 nm [185]. The permeability alterations were wavelength-dependent and followed O_2 absorption. The results are partially reproduced in a review by Zakharov and Ivanov [108]. In connection with these biological results, and as it occurred to the 633 nm dimol band, the 577 nm dimol shows a fortuitous overlap with a monomol band at ~580 nm [183]. This monomol corresponds to the initial excitation of $^1O_2$ (b) v = 3 [186,187]. Authors of ref 108 and 185. advanced that, most probably, the combination of both monomol and dimol absorption explained the observed effect on red blood cells.

4.3.3. Other dimol bands

There are other dimol absorption bands in the visible and the near UV (see Table 1). I am just going to mention them, but not develop them further. This is because more and more compounds absorb light when irradiation wavelengths become shorter, and it becomes a formidable task to assign a single causal agent to a given biological response. In the green spectral region (~532 nm) there is a third dimol band ($[^3O_2 - {}^3O_2] + h\nu \rightarrow [^1O_2\ v = 2 - {}^1O_2\ v = 0]$). Frequency-doubled Nd-based lasers emit at 532 nm and thereby are excellent sources to excite this band. A fourth dimol band exists at ~495 nm ($[^3O_2 - {}^3O_2] + h\nu \rightarrow [^1O_2\ v = 3 - {}^1O_2\ v = 0]$). Another dimol absorption occurs around 477 nm ($[^3O_2 - {}^3O_2] + h\nu \rightarrow [^1O_2\ v = 0 - {}^1O_2\ (b)\ v = 0]$). It has the particularity that both the first and second excited singlet states are simultaneously produced after photon absorption. Further dimol bands can be observed at 446, 420, 395, 380, 360, and 344 nm. They are the result of different combinations of $^1O_2$ and $^1O_2$ (b) being produced in different vibrational states (see Table 1). These bands overlap with a large cohort of endogenous biological chromophores and, from my point of view, offer little advantage in redox biology research due to the complexity of photochemical reactions that can take place. Nevertheless, it can be instructing to mention all these wavelengths for the interested reader.

5. Outlook

In what follows, I will briefly discuss some research and applied concepts to be taken into account when direct optical excitation of O_2 is implemented in redox biology studies. Also I will include comments and suggestions in regards to some scientific areas that share methodological aspects with this technique, introducing different points of view to answer some issues in those areas. To complement this section, the absorption coefficients for $^3O_2$ in several biologically-relevant solvents, recently published, are listed in Table 4. With this data researchers can estimate order-of-magnitude $^1O_2$ production rates and doses, when considering and planning redox biology experiments using direct optical excitation of $^1O_2$.

Table 4
$^3O_2$ absorption coefficients for some wavelengths in different solvents. Data for H_2O and other biologically-relevant solvents are provided with corresponding references.

Solvent	Wavelength	Abs. coefficient ($10^{-3}\ M^{-1}\ cm^{-1}$)	Reference
H_2O	1273 nm	1.5	[107]
	765 nm	1.1	[107]
H_2O + 0.2 M SDS	1270 nm	1.2	[105]
	760 nm	1.0	[105]
D_2O	764.3 nm	1.34	[46]
Ethanol	1270 nm	2.2	[105]
	1273 nm	2.8	[107]
	760 nm	0.97	[105]
	765 nm	1.06	[107]
Acetone	1270 nm	2.3	[105]
	1273 nm	3.2	[106]
	1273 nm	2.9	[107]
	760 nm	0.88	[105]
	765 nm	0.88	[106]
	765 nm	0.96	[107]
	763.6 nm	0.88	[46]
Methanol	764 nm	0.71	[46]

5.1. Methodological aspects of direct optical $^1O_2$ excitation

The direct excitation of $^1O_2$ allows for robust and essential control experiments to be done. This is a strong methodological asset of this approach, and adequate comparison among experimental conditions must be implemented by all means, if one is to conclude the causal role of $^1O_2$ in the biological experiments. These control experiments are affordable due to several reasons. First, if $^1O_2$ is at the origin of a given biological response, then a strong wavelength-dependent effect should be observed. In other words, the response should diminish, and finally disappear, the farther the exciting light is from the peak of the absorption band. This has been observed, for example, when HeLa cells were efficiently damaged under 765 nm excitation, but no deleterious effect was observed once the exciting laser was tuned farther than 15 nm to each side of the 765 nm absorption peak [32]. Similar control-light examples in chemical and biochemical experiments have been done recently by Krasnovsky *et al.* [105–107,110–114]. Thus, this photonic methodology allows for control-light experiments under the same experimental conditions by just changing the wavelength. In fact, redox biology experiments done under this methodological approach should always provide for a sham-irradiation control done at as-close-as-possible wavelengths to the one producing $^1O_2$ (*e.g.* using light at 775 or 780 nm along the “active” 760–765 nm). Oxygen bands are very narrow in comparison to other chromophores which may overlap in absorption (including thermal effects by water excitation). Therefore, biological responses observed under light excitation outside the O_2 bands should make the experimenter suspicious about the possibility that another chromophore is actually the source of the biological outcome.

A second important advantage is that $^1O_2$ lifetime can be modulated, to a certain extent, by several chemical compounds. On one side $^1O_2$ lifetime can be enhanced in living systems by D_2O addition. The energy transfer to D_2O is much less efficient than to H_2O. The lifetime in pure D_2O is ~68 μs [46] in comparison to the 3–4 μs in H_2O. However due to chemical reactions and physical interactions it is of the order of 35 μs in the intracellular milieu [47,48]. In any case this order of magnitude increase in lifetime affords for a noticeable enhancement of $^1O_2$ biological impact: time for necrotic cell killing was reduced four times in D_2O-based incubation medium [32]. On the other side $^1O_2$ lifetime can be reduced by addition of physical and/or chemical quenchers, so that its biological action is diminished. The compound NaN_3 is able to deactivate $^1O_2$ without engaging into chemical reaction. The decay is accompanied by heat release. Unfortunately NaN_3 is poisonous for the mitochondrial electron transport chain but cells tolerate mM final concentrations for several hours. Adequate NaN_3 controls should provide for biological effects due to this compound. Cell media made of different mixing percentages of H_2O:D_2O can also provide for different rates of physical $^1O_2$ quenching, therefore providing insight into $^1O_2$ biological action. Finally several compounds react directly with $^1O_2$ in a sacrificial way, being oxidized themselves instead of cellular components. However results with these compounds should be interpreted with care, as new ROS can form precisely due to these very chemical reactions. For example, ascorbate reacts with $^1O_2$ leading to the production of the superoxide anion radical and H_2O_2 [61].

Most biological studies done so far rely on lasers to excite directly O_2 (for the reasons behind this see Section 5.3 below). Due to the high

coherence and directivity of lasers, it is possible to focus the light beams almost to the diffraction limit. For the wavelengths discussed in this review this means that light spots in the 0.5–1 μm diameter range are affordable. In turn this translates into a very high spatial control over the subcellular domain where $^1O_2$ is being produced. This control opens the way to study subcellular effects driven by $^1O_2$ by irradiating particular organelles or areas. It also allows for studies on the diffusion of $^1O_2$ inside the cell and the differences/similarities of intracellular vs. extracellular generated $^1O_2$ [32]. Something to consider is that the diffraction spot dimensions are commonly referred to the lateral (x and y axis) ones. The depth (z-axis) limit is larger as the beam focuses and then defocuses above and below the focusing spot. In consequence, there is a roughly conical volume above and below the focusing spot where $^1O_2$ is directly excited too [33]. An interesting experiment partly avoiding this issue would be to make use of the total internal reflection effect at an adequate wavelength, to study $^1O_2$ production in a very thin slice just outside/inside the cell. This can be an adequate approach to study the impact of $^1O_2$ on the plasmatic membrane, membrane proteins and receptors, etc. Also to take into account is the fact that actinic light gets scattered and diffracted, especially in cellular environments that show refraction index changes and micrometric structures. As direct $^1O_2$ excitation is a one-photon process this scattered light will produce some $^1O_2$ outside the region of interest.

To avoid unwanted and interfering results due to non-linear optical effects, the use of pulsed lasers should be avoided whenever possible. Biphotonic or multiphotonic excitation because of short laser pulses (nanosecond or shorter) can lead to excitation of organic chromophores (which can photosensitize $^1O_2$ but also other ROS as in the classical photodynamic effect) [34] or induce plasma generation that produces a number of ROS [188]. These effects obscure the role $^1O_2$ can play in redox biology by adding additional parameters the researcher must account for.

5.2. Redox biology with optically excited $^1O_2$

Direct excitation of $^1O_2$ can be employed to induce cellular redox eustress (stimulation [5]) [33,180], redox distress (stress response and damage [5]) [28,33,119,120], cell death [24,27,32,33,116], and, seemingly, it can be put to clinical use, at least for some kind of tumors [108,189]. A puzzling aspect of $^1O_2$ action at all this levels is the apparent high biological susceptibility to small $^1O_2$ amounts: given the very small absorption coefficient of $^3O_2$ and its low concentration in cells and tissues, it is not easy to understand how relatively short irradiations can have such a biological impact. To answer this question is, in my opinion, one of the biggest issues to deal with in regards to $^1O_2$ action in redox biology. A mechanism that can partly address this is the ROS-induced ROS release (RIRR) phenomenon, a term initially introduced to explain the observed chronic increase in ROS production by mitochondria well after an initial oxidative insult has been applied [190,191]. In many of the original studies on RIRR the oxidative treatment was ionizing radiation. In RIRR certain oxidative modifications of the affected mitochondria induce leaks and a faulty behavior in the respiratory process. As a consequence, more ROS are produced by the mitochondria, which in turn deal more oxidative damage and further the inefficient respiration process. This positive feedback perpetuates the deleterious cycle which can end by killing the cell or transforming it. Photoaging processes related to RIRR are known to be driven by $^1O_2$ [73]. Recently the process has been expanded to explain similar events not exclusively linked to mitochondrial ROS production [192]. That an initial “oxidative spark” by optically excited $^1O_2$ can reach the threshold for significant local structural/functional modifications, that subsequently lead to an increased ROS production, seems feasible in view our current knowledge of the cell physiology and RIRR. Putative ROS sources for such an $^1O_2$-driven RIRR can be the mitochondria [28,193], the family of NAD(P)H Oxidases (NOX) [41,194], the lipoxygenases [195] or, most probably, a mixture of all of them. The ROS interconversion process is surely playing a role in this $^1O_2$ susceptibility, as it can transform a short-lived ROS like $^1O_2$ into longer lived species like H_2O_2. In fact, it has been reported that the bystander effect after a photodynamic treatment is mediated by H_2O_2 [196] and other diffusing mediators like lipid peroxidation products [197]. The group led by Rafailov has modelled the impact of an initial $^1O_2$ pool (generated by 1270 nm light exposure) on the subsequent ROS increased production and redox stress in normal and tumoral cells [27,119]. Recently, it has been proposed that extracellular generation of $^1O_2$ can, under the right circumstances, derive into even more $^1O_2$ production through enzymatic processes and catalase inactivation at the cell membrane [194].

It is interesting to remark the potential importance of lipid oxidation products as signaling and damaging agents. Lipids are the bulk components of biological membranes. Oxygen solubility is higher in organic hydrophobic solvents so its concentration is more elevated in biological membranes. At the same time, $^1O_2$ lifetime is longer in this kind of solvents and it is reactive towards lipidic compounds [83,84]. Therefore, it can be expected that lipid oxidation products derived from $^1O_2$ membrane reactions will be one of the main oxidation products to be generated during and right after exposure to one of the actinic wavelengths presented. A particular compound within these oxidation products, 4-hydroxynonenal (4-HNE), has some interesting properties that can partly explain the paradoxical low-dose vs. high-dose biological effects of $^1O_2$. At high doses 4-HNE is cytotoxic and mutagenic, promotes lipid oxidation chain reactions and, due to its amphiphilic aldehyde character, can diffuse from membranes to other cellular locations through the aqueous compartments [86–89,198], also supporting the bystander effect. However, it has been reported that at low doses (micromolar or lower) 4-HNE has physiological signaling roles, like cell mitosis regulation and enhancement [199–201]. Deeping in the mechanisms behind this cell stimulation Ramana *et al.* found activation of protein kinase C, NF-kB and AP-1 after low concentration 4-HNE exposure [202]. Another two groups have found activation of the Src kinase pathway under similar circumstances [203,204]. Mild photodynamic treatments induce cell stimulation partly through activation of Src kinase [41–43], which is a prototypical example of kinase regulation by redox modulation [97]. Intracellular levels of 4-HNE modulate GSH concentration and, in consequence, the overall reduction potential (E_{red}) of the cell [200,202,205]. Additionally, 4-HNE and other lipid oxidation products can increase ROS production by interfering with the mitochondria [88] or NOX [206]. This brings again the RIRR argument introduced previously in this section. In summary, lipid oxidation products, in particular 4-HNE, may work as efficient signal transducers for $^1O_2$-driven redox processes in the cell.

An experimental principle to keep always in mind is that direct optical excitation of $^1O_2$ guarantees that the only ROS produced in the first place is $^1O_2$. As obvious as this might sound, it can help answer fundamental questions in redox biology. For example, in connection to the RIRR phenomenon just discussed or the ROS interconversion processes presented. Does redox signaling show ROS-specificity or is it supported by an unspecific action mechanism? It seems that subtle general modulation of the cellular E_{red} explains many redox signaling effects [19,20,207,208]. As (E_{red}) is tightly dependent on the ratio GSH:GSSG [3,20,78], it is reasonable to think that different cell responses can be obtained by judiciously providing different “oxidative levels”, irrelevant of the particular ROS involved in the induction of the oxidative action, but attending to the location, amount and duration of them. This is, at the moment, highly speculative, but it has been systematically proved that different ROS (H_2O_2, $\bullet O_2^-$ or $^1O_2$) induce very similar cell responses [2,5,18,209].

Following this theoretical argument, a schematic of two opposite cell responses (mitosis stimulation vs. apoptosis) that can be induced by direct optical $^1O_2$ excitation is shown in Fig. 5. The interphase rest cell state is shown in Fig. 5A. Differences exist in the E_{red} value among different cell domains. These have been represented as a color code:

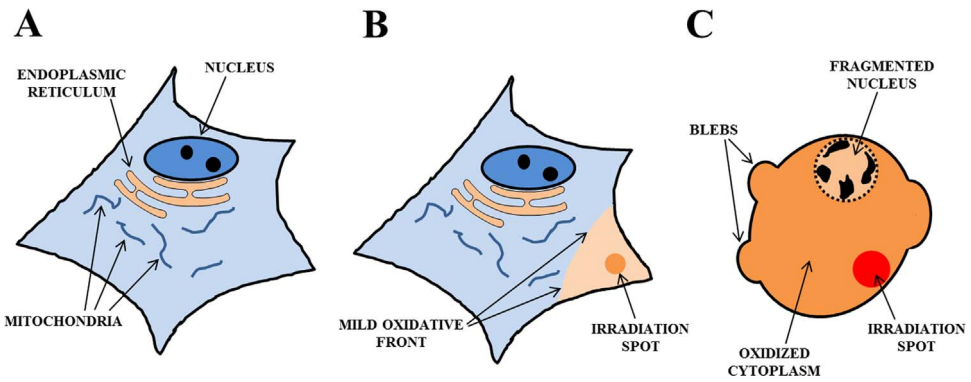

Fig. 5. Model for $^1O_2$ biological modulation depending on the actinic light dose. (A) Under physiological conditions, the cell redox potential is different among cellular organelles. The nucleus and mitochondria show strongly reducing environments (deep blue). The cytoplasm has moderately reducing conditions (light blue), and the endoplasmic reticulum is mildly oxidizing (light orange). (B) When low amounts of $^1O_2$ (deep orange) are produced by a subcellular optical beam (irradiation spot), a transient mild oxidative wave (light orange) diffuses from this location. This can led to engagement of redox signaling pathways (*e.g.* Src kinase), and to biological responses of interest in redox biology. (C) When large amounts of $^1O_2$ (red) are generated, either by a strong light flux or by a long exposure time, a general cytoplasmic oxidation sets in (deep orange), which signals for pathological responses. In this scheme, the irradiated cell is undergoing apoptosis. The nucleus also shows a turn towards oxidative conditions (light orange), the nuclear membrane has dissolved, and chromatin appears condensed and fragmented (*karyorrhexis*). Adapted from [33,210].

cooler colors for more negative E_{red} (more reduced) and warmer for less negative (more oxidized) values. The nucleus, for example, shows a reduced environment (deep blue) to preserve genetic material against oxidative modifications. When a low dose optical treatment is applied to a subcellular spot (Fig. 5B), low amounts of $^1O_2$ are produced that locally decrease the E_{red} value (deep orange spot). ROS diffusing from this spot induce a mild oxidative wave (light orange) that spreads to nearby cell locations. Under the right time-dose conditions, this ROS wave can be transduced to a mitotic signal [21,33,41,210]. If the irradiation is continued and/or the light dose is high enough (Fig. 5C), the amount of ROS in the illuminated spot becomes large (red spot) and a generalized oxidative state imposes in the intracellular milieu (deep orange cytoplasm and light orange nucleus). In this particular case, the irradiated cell is shown undergoing apoptosis. Optical excitation of $^1O_2$ offers the additional possibility to study the alternative biological outcomes of irradiating different intracellular domains and structures/organelles. Interesting results in this area have already been reported using a more classical photodynamic approach irradiating different cytoplasmic areas [211], and ionizing radiation at mitochondria [190].

5.3. Light sources

The most adequate light sources for direct optical excitation of $^1O_2$ are lasers. Several are the arguments underpinning this statement. Lasers produce quite monochromatic light. This means they emit almost pure colors (*i.e.* at a single wavelength). As O_2 absorbs in such narrow bands it is reasonable to pump also with a narrow wavelength source, to avoid wasting most of the light not "tuned" to O_2. Lasers can be cw or pulsed. Both kinds can provide very useful results by direct O_2 excitation. As mentioned previously, for most redox biological experiments cw lasers are better suited as non-linear optical effects are avoided. Some lasers are tunable (*e.g.* Ti:sapphire) which is even more suited because experiments both at actinic and control wavelengths can be accomplished in a simpler setup. These light sources can be very powerful emitting powers from several watts for cw lasers to gigawatts/terawatts for fs pulsed ones. These optical powers, combined with monochromaticity, ensure that shorter times are necessary to achieve biological responses. For microscopic studies (*e.g.* single cell experiments) the coherence of laser light allow for focusing nearly to the diffraction limit. For visible wavelengths, this puts the limit below a micron under optimal conditions.

Many different laser types have been employed to directly pump monomol and dimol O_2 bands: Nd:YAG and Nd-based [29,30,-122–128,135–144], Yb-based [31], He-Ne [29,99,108,123,141,143,144,177–181], semiconductor (diode) [27,108,109,114,119,120,137,146,148–154,168], Raman-shifted [23–26,28,115], dye-based [174,185], alexandrite ($Cr:BeAl_2O_4$) [108], and forsterite ($Cr:Mg_2SiO_4$) [109] to name the most common ones (more examples can be found in each wavelength subsection above). Visible excitation of O_2 has the drawback of overlapping with endogenous cellular chromophores, like cytochromes, porphyrins, certain cofactors (like flavin- and nicotinamide-containing metabolites), etc [170]. Therefore NIR excitation (690–1270 nm) is preferable to avoid complex results. However, wavelengths above ~950 nm excite directly the vibrational overtones of H_2O which leads to sample heating [121,212]. This can be adequately dealt with doing the right experimental controls. But, given that some excitation wavelengths (690–920) fall between these two spectral regions (the so-called optical biological/therapeutic window [15,68,69]), it is reasonable to suggest their use for redox biology studies. Furthermore, absorption coefficients for 810 and 690 nm are very low, which leaves 760 and 920 nm as the best suited bands for these kind of studies. Absorption at 760 nm is stronger than at 920 nm [103], which explains that some recent reports have been done at this wavelength [32–34].

Other light sources have been shown to directly photoexcite O_2, but different features like polychromaticity, low power, incoherence, etc. make them much less suitable than lasers for the topic of this review. LEDs are probably the second best option to obtain $^1O_2$. Recent publications have reported on the feasibility of this approach [146,213–215]. It will be interesting to see the practical importance of these light sources, although they can be adequate for low $^1O_2$ dose studies like those studying biological stimulation [146]. As a historical remark Evans was able to produce $^1O_2$ by optical excitation employing halogens lamps and narrow-band filters to isolate O_2 excitation bands from the blackbody lamp spectrum [99].

5.4. Fluorescence microscopy

Light has an assessing, relatively passive role in fluorescence microscopy by exciting some fluorophore of interest. It turns out, however, that it can excite many other unwanted chromophores. Given the narrow and weak absorption bands of O_2 in the visible, the concerns should be towards organic molecules capable of absorption, not to oxygen. As such, most undesirable oxidative action occurring in fluorescence microscopy is due the classical photodynamic effect or other photochemical reactions. However, currently it is possible to excite in the far red/NIR and record the fluorescent emission in the NIR. Thus, fluorophores excited around 690 nm and 760 nm should be discarded in favor of others or changing the excitation wavelengths.

Non-linear excitation fluorescence microscopy makes much common use of NIR wavelengths [216,217]. Following the same arguments presented above, O_2 absorption bands should be avoided to preserve sample integrity. In this particular field excitation with Ti:sapphire pulsed lasers is very common. Care must be taken not to excite at ~760 nm, ~810 nm or ~920 nm. Additionally, it can be a good idea to use some kind of antioxidant compound (1,4-diazabicyclo[2.2.2]octane –DABCO- is a useful option) or antioxidant fluorescence medium to quench ROS action during sample imaging. This will depend on viability issues, but it is worth assessing its usefulness. This also applies to linear excitation fluorescence microscopy.

Finally it can be interesting to try to detect $^1O_2$ phosphorescence at ~1270 nm after direct excitation at 760 nm in living samples [10,32,37,46]. This is difficult because of the low amount of $^1O_2$ produced in the first place and the very low rate of light emission, especially in the reduced environment that defines living systems. The probability of solvent quenching by H_2O or chemical reaction leave small margin for light emission. Photon detection at 1270 nm requires dedicated equipment but this has been already proved with a classical photodynamic excitation of $^1O_2$ in living cells [47].

5.5. Optical traps

As repeatedly mentioned in Section 4 a significant part of the damage observed with optical tweezers/traps can be assigned to $^1O_2$ directly excited by NIR light [30,135,139,163,164]. The different action spectra reported for deleterious biological action with optical traps clearly fits to the $^3O_2$ absorption spectrum [136–138,142,145,161,218]. Therefore, researchers should refrain of using those wavelengths that fall within the O_2 absorption bands (*i.e.* 760 nm, 810 nm, 920 nm, and 1065 nm). Use of antioxidants and quenchers can be useful ways of minimizing the effect of any $^1O_2$ eventually produced, as long as they do not have negative effects on the samples or these are dealt with adequately with proper controls. At least in one case pre-irradiation at 632.8 nm was employed to “prime” cells for later exposure to 1064 nm light. Cells exposed to 632.8 nm endured better the subsequent irradiation to 1064 nm [141]. Alternatively, optical tweezers working with actinic light can be put to use to assess non-adherent cell redox responses. The cell can be trapped and exposed to $^1O_2$ at the same time. An interesting possibility is to study biomechanical aspects, like cell membrane fluidity or intracellular viscosity during trapping, as the optical tweezers can induce controlled mechanical forces on the cell. Changes in these properties can be correlated to the light flux and the $^1O_2$ dose. Certainly, large viscosity changes have already been reported in relation to photodynamic treatments of cultured cells [219].

5.6. Thermal aspects

Finally, some comments on thermal aspects seem appropriate. Due to the very high light intensities and/or focusing, it is reasonable to assume that very high thermal loads should happen under most experimental situations described. However, absorption by H_2O is relatively low below 1300 nm and almost negligible below 950 nm (biological window) [121]. Unless some exogenous strongly absorbing compound/structure (e.g. nanoparticles) has been introduced in the studied system, water should be the main concern in regards to thermal side effects. This issue has been both theoretically modelled and experimentally measured for different wavelengths and situations [220–222]. Consensus is that the temperature increase in the focal plane is around 1 °C for every 100 mW of light power at 1064 nm. Making use of shorter wavelengths (760 or 920 nm) should reduce the thermal load by at least one order of magnitude. Although heat-driven damage seems not to be a factor of concern, assuming the previous arguments, it is nevertheless important to be aware that some biological effects can have a thermal origin in some redox experiments using light [223–229]. Under certain circumstances, ironically, thermal damage can be an asset. For example, Yusupov et al. reported on the efficient clinical treatment of skin tumors making use of a laser emitting at 1262 nm [23]. The authors assign the main toxic action on the lesions to the production of $^1O_2$, but thermal synergy could not be discarded. Therefore, a combination of oxidative damage and thermal stress can significantly enhance the clinical outcome of certain phototherapies [230].

6. Summary

Direct optical excitation of O_2 for redox biology seems a promising and very productive research area. Definitively, it is a highly interdisciplinary field, which requires inputs from redox biology, biophotonics, physical chemistry, physics, etc. At the same time, it can help respond questions and define new parameters, with the potential to shed light upon many biomedical topics, from ROS-induced pathologies to regenerative processes. It is one of the goals of this review to have introduced the general methodology to the broad audience of researchers in redox biology and photobiology; and, hopefully, to have sparked interest in them about its potentials and further developments.

Conflict of interest

The author declares no conflict of interest.

Acknowledgements

I would like to acknowledge very fruitful discussions, long-term support and critic feedback from Prof. Juan Carlos Stockert, Dr. Begoña López, Dr. Elisa Carrasco and Antonio Romero. Additional support and feedback has been provided by Prof. Peter R. Ogilby and Dr. Thomas Breitenbach. I am thankful to Mikkel Bregnhøj and Michael Westberg for stimulating conversations on this topic too. Experimental work with cw laser sources is acknowledged to Prof. Daniel Jaque and Dr. Patricia Haro. Very constructive comments and suggestions from the reviewers are acknowledged. Prof. Arturo Morales is acknowledged for logistic support. This research did not receive any specific grant from funding agencies in the public, commercial, or not-for-profit sectors.

References

[1] N. Lane, Oxygen: The Molecule That Made the World, Oxford University Press, New York USA, 2002.
[2] W.A. Pryor, K.N. Houk, C.S. Foote, J.M. Fukuto, L.J. Ignarro, et al., Free radical biology and medicine: it's a gas, man!, Am. J. Physiol. Regul. Integr. Comp. Physiol. 291 (2006) R491–R511, http://dx.doi.org/10.1152/ajpregu.00614.2005.
[3] W. Dröge, Free radicals in the physiological control of cell function, Physiol. Rev. 82 (2002) 47–95, http://dx.doi.org/10.1152/physrev.00018.2001.
[4] B. Kalyanaraman, Teaching the basics of redox biology to medical and graduate students: oxidants, antioxidants and disease mechanisms, Redox Biol. 1 (2013) 244–257, http://dx.doi.org/10.1016/j.redox.2013.01.014.
[5] H. Sies, Hydrogen peroxide as a central redox signaling molecule in physiological oxidative stress: oxidative eustress, Redox Biol. 11 (2017) 613–619, http://dx.doi.org/10.1016/j.redox.2016.12.035.
[6] C. Schweitzer, R. Schmidt, Physical mechanisms of generation and deactivation of singlet oxygen, Chem. Rev. 103 (2003) 1685–1757, http://dx.doi.org/10.1021/cr010371d.
[7] T.G. Slanger, R.A. Copeland, Energetic oxygen in the upper atmosphere and the laboratory, Chem. Rev. 103 (2003) 4731–4765, http://dx.doi.org/10.1021/cr0205311.
[8] B.F. Minaev, Electronic mechanisms of molecular oxygen activation, Russ. Chem. Rev. 76 (2007) 988–1010, http://dx.doi.org/10.1070/RC2007v076n11ABEH003720.
[9] A.A. Krasnovsky, Primary mechanisms of photoactivation of molecular oxygen, Hist. Dev. Mod. Status Res., Biochem. 72 (2007) 1065–1080, http://dx.doi.org/10.1134/S0006297907100057.
[10] P.R. Ogilby, Singlet oxygen: there is indeed something new under the sun, Chem. Soc. Rev. 39 (2010) 3181–3209, http://dx.doi.org/10.1039/b926014p.
[11] D.E.J.G.J. Dolmans, D. Fukumura, R.K. Jain, Photodynamic therapy for cancer, Nat. Rev. Cancer 3 (2003) 380–387, http://dx.doi.org/10.1038/nrc1071.
[12] B.C. Wilson, M.S. Patterson, The physics, biophysics and technology of photodynamic therapy, Phys. Med. Biol. 53 (2008) R61–R109, http://dx.doi.org/10.

1088/0031-9155/53/9/R01.
[13] C.A. Robertson, D. Hawkins Evans, H. Abrahamse, Photodynamic therapy (PDT): a short review on cellular mechanisms and cancer research applications for PDT, J. Photochem. Photobiol. B: Biol. 96 (2009) 1–8, http://dx.doi.org/10.1016/j.jphotobiol.2009.04.001.
[14] P. Agostinis, K. Berg, K.A. Cengel, T.H. Foster, A.W. Girotti, et al., Photodynamic therapy of cancer: an update, CA Cancer. J. Clin. 61 (2011) 250–281, http://dx.doi.org/10.3322/caac.20114.
[15] J.M. Dąbrowski, L.G. Arnaut, Photodynamic therapy (PDT) of cancer: from local to systemic treatment, Photochem. Photobiol. Sci. 14 (2015) 1765–1780, http://dx.doi.org/10.1039/c5pp00132c.
[16] L.O. Klotz, K.D. Kröncke, H. Sies, Singlet oxygen-induced signaling effects in mammalian cells, Photochem. Photobiol. Sci. 2 (2003) 88–94, http://dx.doi.org/10.1039/b210750c.
[17] A.N. Onyango, Endogenous generation of singlet oxygen and ozone in human and animal tissues: mechanisms, biological significance, and influence of dietary components, Oxid. Med. Cell. Longev. (2016) 2398573, http://dx.doi.org/10.1155/2016/2398573.
[18] M.J.C. Long, J.R. Poganik, S. Ghosh, Y. Aye, Subcellular redox targeting: bridging *in Vitro* and *in Vivo* chemical biology, ACS Chem. Biol. 12 (2017) 586–600, http://dx.doi.org/10.1021/acschembio.6b01148.
[19] J. Boonstra, J.A. Post, Molecular events associated with reactive oxygen species and cell cycle progression in mammalian cells, Gene 337 (2004) 1–13, http://dx.doi.org/10.1016/j.gene.2004.04.032.
[20] M. Kemp, Y.M. Go, D.P. Jones, Nonequilibrium thermodynamics of thiol/disulfide redox systems: a perspective on redox systems biology, Free Rad. Biol. Med. 44 (2008) 921–937, http://dx.doi.org/10.1016/j.freeradbiomed.2007.11.008.
[21] A. Blázquez-Castro, T. Breitenbach, P.R. Ogilby, Singlet oxygen and ROS in a new light: low-dose subcellular photodynamic treatment enhances proliferation at the single cell level, Photochem. Photobiol. Sci. 13 (2014) 1235–1240, http://dx.doi.org/10.1039/c4pp00113c.
[22] F. Anquez, A. Sivéry, I. El Yazidi-Belkoura, J. Zemmouri, P. Suret, et al., Chapter 4: Production of singlet oxygen by direct photoactivation of molecular oxygen, in: S. Nonell, C. Flors (Eds.), Singlet Oxygen: Applications in Biosciences and Nanosciences, Volume 1, Ch. 4, Comprehensive Series in Photochemical & Photobiological Sciences, Royal Society of Chemistry, 2016. DOI: https://dx.doi.org/10.1039/9781782622208-00075.
[23] A.S. Yusupov, S.E. Goncharov, I.D. Zalevskii, V.M. Paramonov, A.S. Kurkov, Raman fiber laser for the drug-free photodynamic therapy, Laser Phys. 20 (2010) 357–359, http://dx.doi.org/10.1134/S1054660×10040134.
[24] F. Anquez, I. El Yazidi-Belkoura, S. Randoux, P. Suret, E. Courtade, Cancerous cell death from sensitizer free photoactivation of singlet oxygen, Photochem. Photobiol. 88 (2012) 167–174, http://dx.doi.org/10.1111/j.1751-1097.2011.01028.x.
[25] M.R. Detty, Direct 1270 nm irradiation as an alternative to photosensitized generation of singlet oxygen to induce cell death, Photochem. Photobiol. 88 (2012) 2–4, http://dx.doi.org/10.1111/j.1751-1097.2011.01047.x.
[26] T.P. Gening, O.S. Voronova, D.R. Dolgova, T.V. Abakumova, I.O. Zolotovskii, et al., Analysis of the efficiency of using 1265-nm cw laser radiation for initiating oxidative stress in the tissue of a solid malignant tumour, Quant. Electron. 42 (2012) 805–807, http://dx.doi.org/10.1070/QE2012v042n09ABEH014961.
[27] S.G. Sokolovski, S.A. Zolotovskaya, A. Goltsov, C. Pourreyron, A.P. South, et al., Infrared laser pulse triggers increased singlet oxygen production in tumour cells, Sci. Rep. 3 (2013) 3484, http://dx.doi.org/10.1038/srep03484.
[28] Y.V. Saenko, E.S. Glushchenko, I.O. Zolotovskii, E. Sholokhov, A. Kurkov, Mitochondrial dependent oxidative stress in cell culture induced by laser radiation at 1265 nm, Lasers Med. Sci. 31 (2016) 405–413, http://dx.doi.org/10.1007/s10103-015-1861-z.
[29] N.N. Houreld, H. Abrahamse, Cellular damage in diabetic wounded fibroblast cells following phototherapy at 632.8, 830, and 1064 nm, Laser Chem. (2007) 80536, http://dx.doi.org/10.1155/2007/80536.
[30] M.P. Landry, P.M. McCall, Z. Qi, Y.R. Chemla, Characterization of photoactivated singlet oxygen damage in single-molecule optical trap experiments, Biophys. J. 97 (2009) 2128–2136, http://dx.doi.org/10.1016/j.bpj.2009.07.048.
[31] T. Aabo, I.R. Perch-Nielsen, J.S. Dam, D.Z. Palima, H. Siegumfeldt, et al., Effect of long- and short-term exposure to laser light at 1070 nm on growth of *Saccharomyces cerevisiae*, J. Biomed. Opt. 15 (2010) 041505, http://dx.doi.org/10.1117/1.3430731.
[32] M. Bregnhøj, A. Blázquez-Castro, M. Westberg, T. Breitenbach, P.R. Ogilby, Direct 765 nm optical excitation of molecular oxygen in solution and in single mammalian cells, J. Phys. Chem. B 119 (2015) 5422–5429, http://dx.doi.org/10.1021/acs.jpcb.5b01727.
[33] M. Westberg, M. Bregnhøj, A. Blázquez-Castro, T. Breitenbach, M. Etzerodt, et al., Control of singlet oxygen production in experiments performed on single mammalian cells, J. Photochem. Photobiol. A: Chem. 321 (2016) 297–308, http://dx.doi.org/10.1016/j.jphotochem.2016.01.028.
[34] M. Westberg, M. Bregnhøj, C. Banerjee, A. Blázquez-Castro, T. Breitenbach, et al., Exerting better control and specificity with singlet oxygen experiments in live mammalian cells, Methods 109 (2016) 81–91, http://dx.doi.org/10.1016/j.ymeth.2016.07.001.
[35] M. Kasha, A.U. Khan, The physics, chemistry, and biology of singlet molecular oxygen, Ann. N.Y. Acad. Sci. (1970) 5–23, http://dx.doi.org/10.1111/j.1749-6632.1970.tb39294.x.
[36] D.R. Kearns, Physical and chemical properties of singlet molecular oxygen, Chem. Rev. 71 (1971) 395–427, http://dx.doi.org/10.1021/cr60272a004.
[37] D. Weldon, T.D. Poulsen, K.V. Mikkelsen, P.R. Ogilby, Singlet sigma: the “other” singlet oxygen in solution, Photochem. Photobiol. 70 (1999) 369–379, http://dx.doi.org/10.1111/j.1751-1097.1999.tb08238.x.
[38] E.L. Clennan, A. Pace, Advances in singlet oxygen chemistry, Tetrahedron 61 (2005) 6665–6691, http://dx.doi.org/10.1016/j.tet.2005.04.017.
[39] N.A. Romero, D.A. Nicewicz, Organic photoredox catalysis, Chem. Rev. 116 (2016) 10075–10166, http://dx.doi.org/10.1021/acs.chemrev.6b00057.
[40] A.A. Ghogare, A. Greer, Using singlet oxygen to synthesize natural products and drugs, Chem. Rev. 116 (2016) 9994–10034, http://dx.doi.org/10.1021/acs.chemrev.5b00726.
[41] A. Blázquez-Castro, E. Carrasco, M.I. Calvo, P. Jaén, J.C. Stockert, et al., Protoporphyrin IX-dependent photodynamic production of endogenous ROS stimulates cell proliferation, Eur. J. Cell Biol. 91 (2012) 216–223, http://dx.doi.org/10.1016/j.ejcb.2011.12.001.
[42] E. Carrasco, M.I. Calvo, A. Blázquez-Castro, D. Vecchio, A. Zamarron, et al., Photoactivation of ROS production *In Situ* transiently activates cell proliferation in mouse skin and in the hair follicle stem cell niche promoting hair growth and wound healing, J. Invest. Dermatol. 135 (2015) 2611–2622, http://dx.doi.org/10.1038/jid.2015.248.
[43] E. Carrasco, A. Blázquez-Castro, M.I. Calvo, A. Juarranz, J. Espada, Switching on a transient endogenous ROS production in mammalian cells and tissues, Methods 109 (2016) 180–189, http://dx.doi.org/10.1016/j.ymeth.2016.08.013.
[44] B.F. Minaev, Spin-orbit coupling mechanism of singlet oxygen $a^1\Delta_g$ quenching by solvent vibrations, Chem. Phys. 483–484 (2017) 84–95, http://dx.doi.org/10.1016/j.chemphys.2016.11.012.
[45] M. Bregnhøj, P.R. Ogilby, Effect of solvent on the $O_2(a^1\Delta_g) \rightarrow O_2(b^{1\Sigma}{}_g{}^+)$ absorption coefficient, J. Phys. Chem. A 119 (2015) 9236–9243, http://dx.doi.org/10.1021/acs.jpca.5b05131.
[46] M. Bregnhøj, M.V. Kræpøth, R.J. Sørensen, M. Westberg, P.R. Ogilby, Solvent and heavy-atom effects on the $O_2(X^3\Sigma_g{}^-) \rightarrow O_2(b^1\Sigma_g{}^+)$ absorption transition, J. Phys. Chem. A 120 (2016) 8285–8296, http://dx.doi.org/10.1021/acs.jpca.6b08035.
[47] E. Skovsen, J.W. Snyder, J.D.C. Lambert, P.R. Ogilby, Lifetime and diffusion of singlet oxygen in a cell, J. Phys. Chem. B 109 (2005) 8570–8573, http://dx.doi.org/10.1021/jp051163i.
[48] R.W. Redmond, I.E. Kochevar, Spatially resolved cellular responses to singlet oxygen, Photochem. Photobiol. 82 (2006) 1178–1186, http://dx.doi.org/10.1562/2006-04-14-IR-874.
[49] A.P. Wojtovich, T.H. Foster, Optogenetic control of ROS production, Redox Biol. 2 (2014) 368–376, http://dx.doi.org/10.1016/j.redox.2014.01.019.
[50] L. Gao, R. Liu, F. Gao, Y. Wang, X. Jiang, et al., Plasmon-mediated generation of reactive oxygen species from near-infrared light excited gold nanocages for photodynamic therapy *in Vitro*, ACS Nano 8 (2014) 7260–7271, http://dx.doi.org/10.1021/nn502325j.
[51] B.E. Smith, P.B. Roder, J.L. Hanson, S. Manandhar, A. Devaraj, et al., Singlet-oxygen generation from individual semiconducting and metallic nanostructures during near-infrared laser trapping, ACS Photonics 2 (2015) 559–564, http://dx.doi.org/10.1021/acsphotonics.5b00022.
[52] M.L. Brongersma, N.J. Halas, P. Nordlander, Plasmon-induced hot carrier science and technology, Nat. Nanotechnol. 10 (2015) 25–34, http://dx.doi.org/10.1038/NNANO.2014.311.
[53] C.M. Mano, F.M. Prado, J. Massari, G.E. Ronsein, G.R. Martinez, et al., Excited singlet molecular O_2 ($^1\Delta_g$) is generated enzymatically from excited carbonyls in the dark, Sci. Rep. 4 (2014) 5938, http://dx.doi.org/10.1038/srep05938.
[54] M.J. Steinbeck, A.U. Khan, M.J. Karnovsky, Intracellular singlet oxygen generation by phagocytosing neutrophils in response to particles coated with a chemical trap, J. Biol. Chem. 267 (1992) 13425–13433.
[55] C.C. Winterbourn, A.J. Kettle, Redox reactions and microbial killing in the neutrophil phagosome, Antioxid. Redox Signal. 18 (2013) 642–660, http://dx.doi.org/10.1089/ars.2012.4827.
[56] N.J. Turro, M.F. Chow, J. Rigaudy, Mechanism of thermolysis of endoperoxides of aromatic compounds. Activation parameters, magnetic field, and magnetic isotope effects, J. Am. Chem. Soc. 103 (1981) 7218–7224, http://dx.doi.org/10.1021/ja00414a029.
[57] J.M. Aubry, C. Pierlot, J. Rigaudy, R. Schmidt, Reversible binding of oxygen to aromatic compounds, Acc. Chem. Res. 36 (2003) 668–675, http://dx.doi.org/10.1021/ar010086g.
[58] S. Grether-Beck, S. Olaizola-Horn, H. Schmitt, M. Grewe, A. Jahnke, et al., Activation of transcription factor AP-2 mediates UVA radiation- and singlet oxygen-induced expression of the human intercellular adhesion molecule 1 gene, Proc. Natl. Acad. Sci. USA 93 (1996) 14586–14591, http://dx.doi.org/10.1073/pnas.93.25.14586.
[59] C. Pierlot, J.M. Aubry, K. Briviba, H. Sies, P. Di Mascio, Naphthalene endoperoxides as generators of singlet oxygen in biological media, Chapter 1, pp. 3–20, in: Methods in Enzymology, Vol. 319 Singlet Oxygen, UV-A, and Ozone, Academic Press, 2000. DOI: https://dx.doi.org/10.1039/9781782622208-0007510.1016/S0076-6879(00)19003-2.
[60] K. Krumova, G. Cosa, Chapter 1: Overview of reactive oxygen species, in: S. Nonell, C. Flors (Eds.) Singlet Oxygen: Applications in Biosciences and Nanosciences, Volume 1, Ch. 1, Comprehensive Series in Photochemical & Photobiological Sciences, Royal Society of Chemistry, 2016. DOI: https://dx.doi.org/10.1039/9781782622208-0007510.1039/9781782622208-00001.
[61] G.G. Kramarenko, S.G. Hummel, S.M. Martin, G.R. Buettner, Ascorbate reacts with singlet oxygen to produce hydrogen peroxide, Photochem. Photobiol. 82 (2006) 1634–1637, http://dx.doi.org/10.1111/j.1751-1097.2006.tb09823.x.
[62] M. Hayyan, M.A. Hashim, I.M. AlNashef, Superoxide ion: generation and chemical implications, Chem. Rev. 116 (2016) 3029–3085, http://dx.doi.org/10.1021/acs.

chemrev.5b00407.
[63] G. Peters, M.A.J. Rodgers, Single-electron transfer from NADH analogues to singlet oxygen, Biochim. Biophys. Acta Bioenerg. 637 (1981) 43–52, http://dx.doi.org/10.1016/0005-2728(81)90208-5.
[64] I. Saito, T. Matsuura, K. Inoue, Formation of superoxide ion via one-electron transfer from electron donors to singlet oxygen, J. Am. Chem. Soc. 105 (1983) 3200–3206, http://dx.doi.org/10.1021/ja00348a040.
[65] H. Wefers, H. Sies, Oxidation of glutathione by the superoxide radical to the disulfide and the sulfonate yielding singlet oxygen, Eur. J. Biochem. 137 (1983) 29–36, http://dx.doi.org/10.1111/j.1432-1033.1983.tb07791.x.
[66] R.G. Cosso, J. Turim, I.L. Nantes, A.M. Almeida, P. Di Mascio, et al., Mitochondrial permeability transition induced by chemically generated singlet oxygen, J. Bioenerg. Biomembr. 34 (2002) 157–163, http://dx.doi.org/10.1023/A:1016075218162.
[67] C. von Monfort, V.S. Sharov, S. Metzger, C. Schöneich, H. Sies, et al., Singlet oxygen inactivates protein tyrosine phosphatase-1B by oxidation of the active site cysteine, Biol. Chem. 387 (2006) 1399–1404, http://dx.doi.org/10.1515/BC.2006.175.
[68] I.O.L. Bacellar, T.M. Tsubone, C. Pavani, M.S. Baptista, Photodynamic efficiency: from molecular photochemistry to cell death, Int. J. Mol. Sci. 16 (2015) 20523–20559, http://dx.doi.org/10.3390/ijms160920523.
[69] L. Benov, Photodynamic therapy: current status and future directions, Med. Princ. Pract. 24 (2015) 14–28, http://dx.doi.org/10.1159/000362416.
[70] D. Graindorge, S. Martineau, C. Machon, P. Arnoux, J. Guitton, et al., Singlet oxygen-mediated oxidation during UVA radiation alters the dynamic of genomic DNA replication, PLoS One 10 (2015) e0140645, http://dx.doi.org/10.1371/journal.pone.0140645.
[71] J.G. Gao, A. Shih, M. Simon, The role of singlet oxygen in the UVA-induced bystander effect on dermal fibroblasts, FASEB J. 25 (2011) 528.5.
[72] J. Piette, Signalling pathway activation by photodynamic therapy: nf-κb at the crossroad between oncology and immunology, Photochem. Photobiol. Sci. 14 (2015) 1510–1517, http://dx.doi.org/10.1039/C4PP00465E.
[73] M. Berneburg, S. Grether-Beck, V. Kürten, T. Ruzicka, K. Briviba, et al., Singlet oxygen mediates the UVA-induced generation of the photoaging-associated mitochondrial common deletion, J. Biol. Chem. 274 (1999) 15345–15349, http://dx.doi.org/10.1074/jbc.274.22.15345.
[74] J.L. Ravanat, P. Di Mascio, G.R. Martinez, M.H.G. Medeiros, J. Cadet, Singlet oxygen induces oxidation of cellular DNA, J. Biol. Chem. 275 (2000) 40601–40604, http://dx.doi.org/10.1074/jbc.M006681200.
[75] J.L. Ravanat, S. Sauvaigo, S. Caillat, G.R. Martinez, M.H. Medeiros, et al., Singlet oxygen-mediated damage to cellular DNA determined by the comet assay associated with DNA repair enzymes, Biol. Chem. 385 (2004) 17–20, http://dx.doi.org/10.1515/BC.2004.003.
[76] D. Kessel, Autophagic death probed by photodynamic therapy, Autophagy 11 (2015) 1941–1943, http://dx.doi.org/10.1080/15548627.2015.1078960.
[77] D.I. Pattison, A.S. Rahmanto, M.J. Davies, Photo-oxidation of proteins, Photochem. Photobiol. Sci. 11 (2012) 38–53, http://dx.doi.org/10.1039/C1PP05164D.
[78] C. Espinosa-Diez, V. Miguel, D. Mennerich, T. Kietzmann, P. Sánchez-Pérez, et al., Antioxidant responses and cellular adjustments to oxidative stress, Redox Biol. 6 (2015) 183–197, http://dx.doi.org/10.1016/j.redox.2015.07.008.
[79] M.J. Davies, Reactive species formed on proteins exposed to singlet oxygen, Photochem. Photobiol. Sci. 3 (2004) 17–25, http://dx.doi.org/10.1039/B307576C.
[80] J. Cadet, T. Douki, J.L. Ravanat, P. Di Mascio, Chapter 20: Reactions of singlet oxygen with nucleic acids, in: S. Nonell, C. Flors (Eds.) Singlet Oxygen: Applications in Biosciences and Nanosciences, Volume 1, Ch. 20, Comprehensive Series in Photochemical & Photobiological Sciences, Royal Society of Chemistry, 2016. DOI: https://dx.doi.org/10.1039/9781782622208-00393.
[81] M. Yasui, Y. Kanemaru, N. Kamoshita, T. Suzuki, T. Arakawa, et al., Tracing the fates of site-specifically introduced DNA adducts in the human genome, DNA Repair 15 (2014) 11–20, http://dx.doi.org/10.1016/j.dnarep.2014.01.003.
[82] J. Li, A. Braganza, R.W. Sobol, Base excision repair facilitates a functional relationship between guanine oxidation and histone demethylation, Antioxid. Redox Signal. 18 (2013) 2429–2443, http://dx.doi.org/10.1089/ars.2012.5107.
[83] A.W. Girotti, W. Korytowski, Chapter 21: Reactions of singlet oxygen with membrane lipids: lipid hydroperoxide generation, translocation, reductive turnover, and signaling activity, in: S. Nonell, C. Flors (Eds.) Singlet Oxygen: Applications in Biosciences and Nanosciences, Volume 1, Ch. 21, Comprehensive Series in Photochemical & Photobiological Sciences, Royal Society of Chemistry, 2016. DOI: https://dx.doi.org/10.1039/9781782622208-00409.
[84] A.W. Girotti, Photosensitized oxidation of membrane lipids: reaction pathways, cytotoxic effects, and cytoprotective mechanisms, J. Photochem. Photobiol. B: Biol. 63 (2001) 103–113, http://dx.doi.org/10.1016/S1011-1344(01)00207-X.
[85] S. Miyamoto, G.R. Martínez, M.H.G. Medeiros, P. Di Mascio, Singlet molecular oxygen generated by biological hydroperoxides, J. Photochem. Photobiol. B: Biol. 139 (2014) 24–33, http://dx.doi.org/10.1016/j.jphotobiol.2014.03.028.
[86] A.W. Girotti, Translocation as a means of disseminating lipid hydroperoxide-induced oxidative damage and effector action, Free Radic. Biol. Med. 44 (2008) 956–968, http://dx.doi.org/10.1016/j.freeradbiomed.2007.12.004.
[87] M. Hong, A. Xu, H. Zhou, L. Wu, G. Randers-Pehrson, et al., Mechanism of genotoxicity induced by targeted cytoplasmic irradiation, Br. J. Cancer 103 (2010) 1263–1268, http://dx.doi.org/10.1038/sj.bjc.6605888.
[88] H. Zhong, H. Yin, Role of lipid peroxidation derived 4-hydroxynonenal (4-HNE) in cancer: focusing on mitochondria, Redox Biol. 4 (2015) 193–199, http://dx.doi.org/10.1016/j.redox.2014.12.011.
[89] A. Ayala, M.F. Muñoz, S. Argüelles, Lipid peroxidation: production, metabolism, and signaling mechanisms of malondialdehyde and 4-hydroxy-2-nonenal, Oxidat. Med. Cell. Longev. 2014 (2014) 360438, http://dx.doi.org/10.1155/2014/360438.
[90] G.E. Ronsein, M.C.B. De Oliveira, M.H.G. Medeiros, S. Miyamoto, P. Di Mascio, DNA strand breaks and base modifications induced by cholesterol hydroperoxides, Free Radic. Res. 45 (2011) 266–275, http://dx.doi.org/10.3109/10715762.2010.524215.
[91] M. Wlaschek, K. Briviba, G.P. Stricklin, H. Sies, K. Scharffetter-Kochanek, Singlet oxygen may mediate the ultraviolet a-induced synthesis of interstitial collagenase, J. Invest. Dermatol. 104 (1995) 194–198, http://dx.doi.org/10.1111/1523-1747.ep12612751.
[92] M. Wlaschek, J. Wenk, P. Brenneisen, K. Briviba, A. Schwarz, et al., Singlet oxygen is an early intermediate in cytokine-dependent ultraviolet-A induction of interstitial collagenase in human dermal fibroblasts *in vitro*, FEBS Lett. 413 (1997) 239–242, http://dx.doi.org/10.1016/S0014-5793(97)00919-8.
[93] L.O. Klotz, C. Pellieux, K. Briviba, C. Pierlot, J.M. Aubry, et al., Mitogen-activated protein kinase (p38-, JNK-, ERK-) activation pattern induced by extracellular and intracellular singlet oxygen and UVA, FEBS J. 260 (1999) 917–922, http://dx.doi.org/10.1046/j.1432-1327.1999.00255.x.
[94] T.W. Stief, The physiology and pharmacology of singlet oxygen, Med. Hypotheses 60 (2003) 567–572, http://dx.doi.org/10.1016/S0306-9877(03)00026-4.
[95] A.W. Girotti, T. Kriska, Role of lipid hydroperoxides in photo-oxidative stress signaling, Antioxid. Redox Signal. 6 (2004) 301–310, http://dx.doi.org/10.1089/152308604322899369.
[96] P.R. Ogilby, M.K. Kuimova, Chapter 34: Singlet oxygen in mammalian cells, in Singlet Oxygen : Applications in Biosciences and Nanosciences (Ed. S. Nonell, C. Flors), Volume 2, Ch. 34, Comprehensive Series in Photochemical & Photobiological Sciences, Royal Society of Chemistry (2016) DOI: https://dx.doi.org/10.1039/9781782626992-00169.
[97] E. Giannoni, M.L. Taddei, P. Chiarugi, Src redox regulation: again in the front line, Free Radic. Biol. Med. 49 (2010) 516–527, http://dx.doi.org/10.1016/j.freeradbiomed.2010.04.025.
[98] G. Herzberg, Molecular Spectra and Molecular Structure: I. Spectra of Diatomic Molecules, 2nd edition, Van Nostrand Reinhold Company-Prentice Hall, New York, 1950.
[99] D.F. Evans, Oxidation by photochemically produced singlet states of oxygen, J. Chem. Soc. D. (1969) 367–368, http://dx.doi.org/10.1039/C29690000367.
[100] I.B.C. Matheson, J. Lee, Comparison of the pressure dependencies of the visible and infrared electronic absorption spectra of oxygen in gas and in Freon solution, Chem. Phys. Lett. 8 (1971) 173–176, http://dx.doi.org/10.1016/0009-2614(71)80006-4.
[101] D.L. Huestis, G. Black, S.A. Edelstein, R.L. Sharpless, Fluorescence and quenching of $O_2(^1\Delta_g)$ and $[O_2(^1\Delta_g)]_2$ in liquid oxygen, J. Chem. Phys. 60 (1974) 4471–4474, http://dx.doi.org/10.1063/1.1680925.
[102] P.D. Cooper, R.E. Johnson, T.I. Quickenden, A review of possible optical absorption features of oxygen molecules in the icy surfaces of outer solar system bodies, Planet. Space Sci. 51 (2003) 183–192, http://dx.doi.org/10.1016/S0032-0633(02)00205-2.
[103] S. Jockusch, N.J. Turro, E.K. Thompson, M. Gouterman, J.B. Callis, et al., Singlet molecular oxygen by direct excitation, Photochem. Photobiol. Sci. 7 (2008) 235–239, http://dx.doi.org/10.1039/b714286b.
[104] R. Thalman, R. Volkamer, Temperature dependent absorption cross-sections of O_2–O_2 collision pairs between 340 and 630 nm and at atmospherically relevant pressure, Phys. Chem. Chem. Phys. 15 (2013) 15371, http://dx.doi.org/10.1039/c3cp50968k.
[105] A.A. Krasnovsky, A.S. Kozlov, Y. Roumbal, Photochemical investigation of the IR absorption bands of molecular oxygen in organic and aqueous environment, Photochem. Photobiol. Sci. 11 (2012) 988–997, http://dx.doi.org/10.1039/C2PP05350K.
[106] A.A. Krasnovsky, A.S. Kozlov, New approach to measurement of IR absorption spectra of dissolved oxygen molecules based on photochemical activity of oxygen upon direct laser excitation, Biophysics 59 (2014) 199–205, http://dx.doi.org/10.1134/S000635091402016X.
[107] A.A. Krasnovsky, A.S. Kozlov, Photonics of dissolved oxygen molecules. Comparison of the rates of direct and photosensitized excitation of oxygen and reevaluation of the oxygen absorption coefficients, J. Photochem. Photobiol. A: Chem. 329 (2016) 167–174, http://dx.doi.org/10.1016/j.jphotochem.2016.06.026.
[108] S.D. Zakharov, A.V. Ivanov, Light-oxygen effect in cells and its potential applications in tumour therapy (review), Quant. Electron. 29 (1999) 1031–1053, http://dx.doi.org/10.1070/QE1999v029n12ABEH001629.
[109] A.A. Krasnovsky, N.N. Drozdova, A.V. Ivanov, R.V. Ambartsumian, Activation of molecular oxygen by infrared laser radiation in pigment-free aerobic systems, Biochemistry 68 (2003) 963–966, http://dx.doi.org/10.1023/A:1026052310563.
[110] A.A. Krasnovsky, R.V. Ambartzumian, Tetracene oxygenation caused by infrared excitation of molecular oxygen in air-saturated solutions: the photoreaction action spectrum and spectroscopic parameters of the $^1\Delta_g \leftarrow {}^3\Sigma^-_g$ transition in oxygen molecules, Chem. Phys. Lett. 400 (2004) 531–535, http://dx.doi.org/10.1016/j.cplett.2004.11.009.
[111] A.A. Krasnovsky, N.N. Drozdova, Y.V. Roumbal, A.V. Ivanov, R.V. Ambartzumian, Biophotonics of molecular oxygen: activation efficiencies upon direct and photosensitized excitation, Chin. Opt. Lett. 3 (2005) S1–S4.
[112] A.A. Krasnovsky, Y.V. Roumbal, A.V. Ivanov, R.V. Ambartzumian, Solvent dependence of the steady-state rate of $^1O_2$ generation upon excitation of dissolved oxygen by cw 1267 nm laser radiation in air-saturated solutions: estimates of the

absorbance and molar absorption coefficients of oxygen at the excitation wavelength, Chem. Phys. Lett. 430 (2006) 260–264, http://dx.doi.org/10.1016/j.cplett.2006.08.083.
[113] A.A. Krasnovsky, Luminescence and photochemical studies of singlet oxygen photonics, J. Photochem. Photobiol. A: Chem. 196 (2008) 210–218, http://dx.doi.org/10.1016/j.jphotochem.2007.12.015.
[114] A.A. Krasnovsky, Y.V. Roumbal, A.A. Strizhakov, Rates of $^1O_2$ ($^1\Delta_g$) production upon direct excitation of molecular oxygen by 1270 nm laser radiation in air-saturated alcohols and micellar aqueous dispersions, Chem. Phys. Lett. 458 (2008) 195–199, http://dx.doi.org/10.1016/j.cplett.2008.04.091.
[115] F. Anquez, E. Courtade, A. Sivéry, P. Suret, S. Randoux, A high-power tunable Raman fiber ring laser for the investigation of singlet oxygen production from direct laser excitation around 1270 nm, Opt. Express 22 (2010) 22928–22936, http://dx.doi.org/10.1364/OE.18.022928.
[116] F. Anquez, I. El Yazidi-Belkoura, P. Suret, S. Randoux, E. Courtade, Cell death induced by direct laser activation of singlet oxygen at 1270 nm, Laser Phys. 23 (2013) 025601, http://dx.doi.org/10.1088/1054-660X/23/2/025601.
[117] A. Sivéry, F. Anquez, C. Pierlot, J.M. Aubry, E. Courtade, Singlet oxygen ($^1O_2$) generation upon 1270 nm laser irradiation of ground state oxygen ($^3O_2$) dissolved in organic solvents: simultaneous and independent determination of $^1O_2$ production rate and reactivity with chemical traps, Chem. Phys. Lett. 555 (2013) 252–257, http://dx.doi.org/10.1016/j.cplett.2012.10.063.
[118] A. Sivéry, A. Barras, R. Boukherroub, C. Pierlot, J.M. Aubry, et al., Production rate and reactivity of singlet oxygen $^1O_2(^1\Delta_g)$ directly photoactivated at 1270 nm in lipid nanocapsules dispersed in water, J. Phys. Chem. C 118 (2014) 2885–2893, http://dx.doi.org/10.1021/jp412497k.
[119] S.G. Sokolovski, A. Goltsov, E.U. Rafailov, Modelling the hypersensitivity of cancer cells to infra-red laser pulse: breaking ROS defence machinery, in: Proceedings SPIE 8568, Optical Methods for Tumor Treatment and Detection: Mechanisms and Techniques in Photodynamic Therapy XXII, 85680E. DOI: https://dx.doi.org/10.1117/12.2001715, 2013.
[120] E.U. Rafailov, K.S. Litvinova, S.G. Sokolovski, Towards novel compact laser sources for non-invasive diagnostics and treatment, in: Proceedings of SPIE Vol. 9550, Biosensing and Nanomedicine VIII 95500G. DOI: https://dx.doi.org/10.1117/12.2193777, 2015.
[121] G.M. Hale, M.R. Querry, Optical constants of water in the 200-nm to 200-μm wavelength region, Appl. Opt. 12 (1973) 555–563, http://dx.doi.org/10.1364/AO.12.000555.
[122] I.B.C. Matheson, J. Lee, Reaction of chemical acceptors with singlet oxygen produced by direct laser excitation, Chem. Phys. Lett. 7 (1970) 475–476, http://dx.doi.org/10.1016/0009-2614(70)80341-4.
[123] D.F. Evans, J.N. Tucker, Reactivity of the $(^1\Delta_g)_2$ and $^1\Delta_g$ states of oxygen produced by direct laser excitation, J. Chem. Soc. Faraday Trans. 2 (1976) 1661–1666, http://dx.doi.org/10.1039/F29767201661.
[124] I.B.C. Matheson, The absolute value of the reaction rate constant of bilirubin with singlet oxygen in D_2O, Photochem. Photobiol. 29 (1979) 875–878, http://dx.doi.org/10.1111/j.1751-1097.1979.tb07785.x.
[125] L. Skuja, B. Güttler, Detection of interstitial oxygen molecules in SiO_2 glass by a direct photoexcitation of the infrared luminescence of singlet O_2, Phys. Rev. Lett. 77 (1996) 2093–2096, http://dx.doi.org/10.1103/PhysRevLett.77.2093.
[126] I.B.C. Matheson, J. Lee, Observation of the singlet oxygen dimol emission from neodymium laser pumped oxygen in the gas phase and in 1,1,2-trichlorotrifluoroethane solution, Chem. Phys. Lett. 27 (1974) 355–358, http://dx.doi.org/10.1016/0009-2614(74)90240-1.
[127] R. Protz, M. Maier, Laser induced fluorescence and relaxation of singlet molecular oxygen the liquid phase, J. Chem. Phys. 73 (1980) 5464–5467, http://dx.doi.org/10.1063/1.440091.
[128] A. Yamagishi, T. Ohta, J. Konno, H. Inaba, Visible fluorescence of liquid oxygen excited by a Q-switched Nd:YAG laser, J. Opt. Soc. Am. 71 (1981) 1197–1201, http://dx.doi.org/10.1364/JOSA.71.001197.
[129] O.B. Zapol´skiĭ, V.I. Igoshin, A.N. Oraevskiĭ, Feasibility of lasing in collision-induced dipole transitions of molecular oxygen, JETP Lett. 21 (1975) 529–532.
[130] B. Zhadanov, T.L. Henshaw, K. Hobbs, D.K. Neumann, Generation of high densities of gas phase $O_2(a^1\Delta)$ from optical pumping of liquid oxygen, in: Proceedings of Conference on Lasers and Electro-Optics, 2003. CLEO '03, 2003.
[131] R.R. Reibel, J.K. Brasseur, D.K. Neumann, Optically pumped liquid oxygen jet waveguides for production of singlet delta oxygen, in: Proceedings of Conference on Lasers and Electro-Optics, 2004. CLEO '04, 2004.
[132] D.L. Huestis, Challenges for lasers in liquid oxygen, Chem. Phys. Lett. 411 (2005) 108–110, http://dx.doi.org/10.1016/j.cplett.2005.06.029.
[133] A. Kumar, R. Rajesh, G. Singhal, R.K. Tyagi, Analysis of various optical pumping schemes for liquid oxygen lasers, Appl. Phys. B 89 (2007) 385–394, http://dx.doi.org/10.1007/s00340-007-2804-6.
[134] I.B.C. Matheson, J. Lee, Chemical reaction rates of amino acids with singlet oxygen, Photochem. Photobiol. 29 (1979) 879–881, http://dx.doi.org/10.1111/j.1751-1097.1979.tb07786.x.
[135] Y. Liu, G.J. Sonek, M.W. Berns, B.J. Tromberg, Physiological monitoring of optically trapped cells: assessing the effects of confinement by 1064-nm laser tweezers using microfluorometry, Biophys. J. 71 (1996) 2158–2167, http://dx.doi.org/10.1016/S0006-3495(96)79417-1.
[136] H. Liang, K.T. Vu, P. Krishnan, T.C. Trang, D. Shin, et al., Wavelength dependence of cell cloning efficiency after optical trapping, Biophys. J. 70 (1996) 1529–1533, http://dx.doi.org/10.1016/S0006-3495(96)79716-3.
[137] K.C. Neuman, E.H. Chadd, G.F. Liou, K. Bergman, S.M. Block, Characterization of photodamage to *Escherichia coli* in optical traps, Biophys. J. 77 (1999) 2856–2863, http://dx.doi.org/10.1016/S0006-3495(99)77117-1.
[138] S.K. Mohanty, A. Rapp, S. Monajembashi, P.K. Gupta, K.O. Greulich, Comet assay measurements of DNA damage in cells by laser microbeams and trapping beams with wavelengths spanning a range of 308 nm to 1064 nm, Rad. Res. 157 (2002) 378–385, http://dx.doi.org/10.1667/0033-7587(2002)157[0378:CAMODD]2.0.CO;2.
[139] S. Ayano, Y. Wakamoto, S. Yamashita, K. Yasuda, Quantitative measurement of damage caused by 1064-nm wavelength optical trapping of *Escherichia coli* cells using on-chip single cell cultivation system, Biochem. Biophys. Res. Commun. 350 (2006) 678–684, http://dx.doi.org/10.1016/j.bbrc.2006.09.115.
[140] S.K. Mohanty, M. Sharma, P.K. Gupta, Generation of ROS in cells on exposure to CW and pulsed near-infrared laser tweezers, Photochem. Photobiol. Sci. 5 (2006) 134–139, http://dx.doi.org/10.1039/b506061c.
[141] K. Sahu, S.K. Mohanty, P.K. Gupta, He–Ne laser (632.8 nm) pre-irradiation gives protection against DNA damage induced by a near-infrared trapping beam, J. Biophoton. 2 (2009) 140–144, http://dx.doi.org/10.1002/jbio.200810041.
[142] Z. Pilát, J. Ježet, M. Šerý, M. Trtílek, L. Nedbal, et al., Optical trapping of microalgae at 735–1064 nm: photodamage assessment, J. Photochem. Photobiol. B: Biol. 121 (2013) 27–31, http://dx.doi.org/10.1016/j.jphotobiol.2013.02.006.
[143] D. Hawkins-Evans, H. Abrahamse, Efficacy of three different laser wavelengths for *in vitro* wound healing, Photodermatol. Photoimmunol. Photomed. 24 (2008) 199–210, http://dx.doi.org/10.1111/j.1600-0781.2008.00362.x.
[144] N.N. Houreld, H. Abrahamse, Laser light influences cellular viability and proliferation in diabetic-wounded fibroblast cells in a dose- and wavelength-dependent manner, Lasers Med. Sci. 23 (2008) 11–18, http://dx.doi.org/10.1007/s10103-007-0445-y.
[145] U. Mirsaidov, W. Timp, K. Timp, M. Mir, P. Matsudaira, et al., Optimal optical trap for bacterial viability, Phys. Rev. E 78 (2008) 021910, http://dx.doi.org/10.1103/PhysRevE.78.021910.
[146] R. Spitler, M.W. Berns, Comparison of laser and diode sources for acceleration of *in vitro* wound healing by low-level light therapy, J. Biomed. Opt. 19 (2014) 038001, http://dx.doi.org/10.1117/1.JBO.19.3.038001.
[147] G. Leitz, E. Fällman, S. Tuck, O. Axner, Stress response in *Caenorhabditis elegans* caused by optical tweezers: wavelength, power, and time dependence, Biophys. J. 82 (2002) 2224–2231, http://dx.doi.org/10.1016/S0006-3495(02)75568-9.
[148] H. Murayama, K. Sadakane, B. Yamanoha, S. Kogure, Low-power 808-nm laser irradiation inhibits cell proliferation of a human-derived glioblastoma cell line *in vitro*, Lasers Med. Sci. 27 (2012) 87–93, http://dx.doi.org/10.1007/s10103-011-0924-z.
[149] L.P. da Silva Sergio, A.P. Almeida da Silva, P.F. Amorim, V.M. Araújo Campos, L.A. Gonçalves Magalhães, et al., DNA damage in blood cells exposed to low-level lasers, Lasers Surg. Med. 47 (2015) 361–368, http://dx.doi.org/10.1002/lsm.22344.
[150] L.A.S.N. Trajano, L.P.S. Sergio, C.L. Silva, L. Carvalho, A.L. Mencalha, et al., Low-level laser irradiation alters mRNA expression from genes involved in DNA repair and genomic stabilization in myoblasts, Laser Phys. Lett. 13 (2016) 075601, http://dx.doi.org/10.1088/1612-2011/13/7/075601.
[151] L.A. da Silva Neto Trajano, C.L. da Silva, S. Nunes de Carvalho, E. Cortez, A.L. Mencalha, Cell viability, reactive oxygen species, apoptosis, and necrosis in myoblast cultures exposed to low-level infrared laser, Lasers Med. Sci. 31 (2016) 841–848, http://dx.doi.org/10.1007/s10103-016-1909-8.
[152] L.G. Almeida, L.P.S. Sergio, S.C. Vicentini, A.L. Mencalha, F. Paoli, et al., Nuclear phenotype evaluation in skeletal muscle from Wistar rats exposed to low-level lasers, Laser Phys. 27 (2017) 035601, http://dx.doi.org/10.1088/1555-6611/aa5a18.
[153] Z. Yu, Z. Li, N. Liu, Y. Jizhang, T.J. McCarthy, et al., Near infrared radiation protects against oxygen-glucose deprivation-induced neurotoxicity by down-regulating neuronal nitric oxide synthase (nNOS) activity *in vitro*, Metab. Brain Dis. 30 (2015) 829–837, http://dx.doi.org/10.1007/s11011-015-9663-3.
[154] Z. Yu, N. Liu, J. Zhao, Y. Li, T.J. McCarthy, et al., Near infrared radiation rescues mitochondrial dysfunction in cortical neurons after oxygen-glucose deprivation, Metab. Brain Dis. 30 (2015) 491–496, http://dx.doi.org/10.1007/s11011-014-9515-6.
[155] L.R. Martin, R.B. Cohen, J.F. Schatz, Quenching of laser induced fluorescence of O_2 ($b\ ^{1\Sigma+}{}_g$) by O_2 and N_2, Chem. Phys. Lett. 41 (1976) 394–396, http://dx.doi.org/10.1016/0009-2614(76)80838-X.
[156] M.B. Knickelbein, K.L. Marsh, O.E. Ulrich, G.E. Busch, Energy transfer kinetics of singlet molecular oxygen: the deactivation channel for $O_2(b\ ^{1\Sigma+}{}_g)$, J. Chem. Phys. 87 (1987) 2392–2393, http://dx.doi.org/10.1063/1.453120.
[157] J. Wildt, G. Bednarek, E.H. Fink, Laser excitation of O_2 ($b\ ^{1\Sigma+}{}_g$, v´ = 0, 1, 2) – rates and channels of energy transfer and quenching, Chem. Phys. 122 (1988) 463–470, http://dx.doi.org/10.1016/0301-0104(88)80027-2.
[158] S. Xu, D. Dai, J. Xie, G. Sha, C. Zhang, Quantitative measurements of O_2 b ← X (2,1,0←0) bands by using cavity ring-down spectroscopy, Chem. Phys. Lett. 303 (1999) 171–175, http://dx.doi.org/10.1016/S0009-2614(99)00192-X.
[159] S.L. Cheah, Y.P. Lee, J.F. Ogilvie, Wavenumbers, strengths, widths and shifts with pressure of lines in four bands of gaseous $^{16}O_2$ in the systems $a^1\Delta_g$ - $X^{3\Sigma-}{}_g$ and $b^{1\Sigma+}{}_g - X^{3\Sigma-}{}_g$, J. Quant. Spectrosc. Rad. Trans. 64 (2000) 467–482, http://dx.doi.org/10.1016/S0022-4073(99)00126-0.
[160] A. Pohlkötter, M. Köhring, U. Willer, W. Schade, Detection of `opy, Sensors 10 (2010) 8466–8477, http://dx.doi.org/10.3390/s100908466.
[161] I.A. Vorobjev, H. Liang, W.H. Wright, M.W. Berns, Optical trapping for chromosome manipulation: a wavelength dependence of induced chromosome bridges, Biophys. J. 64 (1993) 533–538, http://dx.doi.org/10.1016/S0006-3495(93)81398-5.
[162] K. König, H. Liang, M.W. Berns, B.J. Tromberg, Cell damage by near-IR microbeams, Nature 377 (1995) 20–21, http://dx.doi.org/10.1038/377020a0.

[163] K. König, H. Liang, M.W. Berns, B.J. Tromberg, Cell damage in near-infrared multimode optical traps as a result of multiphoton absorption, Opt. Lett. 21 (1996) 1090–1092, http://dx.doi.org/10.1364/OL.21.001090.
[164] H. Liang, K.T. Vu, T.C. Trang, D. Shin, Y.E. Lee, et al., Giant cell formation in cells exposed to 740 nm and 760 nm optical traps, Lasers Surg. Med. 21 (1997) 159–165, http://dx.doi.org/10.1002/(SICI)1096-9101(1997)21:23.0.CO;2-P.
[165] K. König, P.T.C. So, W.W. Mantulin, E. Gratton, Cellular response to near-infrared femtosecond laser pulses in two-photon microscopes, Opt. Lett. 22 (1997) 135–136, http://dx.doi.org/10.1364/OL.22.000135.
[166] S.A. Lawton, S.E. Novick, H.P. Broida, A.V. Phelps, Quenching of optically pumped $O_2(b^{1\Sigma+}{}_g)$ by ground state O_2 molecules, J. Chem. Phys. 66 (1977) 1381–1382, http://dx.doi.org/10.1063/1.434038.
[167] H.I. Bloemink, R.A. Copeland, T.G. Slanger, Collisional removal of O_2 ($b\ ^{1\Sigma+}{}_g$, v = 1, 2) by O_2, N_2, and CO_2, J. Chem. Phys. 109 (1998) 4237–4245, http://dx.doi.org/10.1063/1.477029.
[168] L. Almeida-Lopes, J. Rigau, R.A. Zângaro, J.J. Guidugli-Neto, M. Martins Marques Jaeger, Comparison of the low level laser therapy effects on cultured human gingival fibroblasts proliferation using different irradiance and same fluence, Lasers Surg. Med. 29 (2001) 179–184, http://dx.doi.org/10.1002/lsm.1107.
[169] T.I. Karu, Mitochondrial signaling in mammalian cells activated by red and near-IR radiation, Photochem. Photobiol. 84 (2008) 1091–1099 (DOI: 10.1111/j.1751-1097.2008.00394.x).
[170] S. Passarella, T. Karu, Absorption of monochromatic and narrow band radiation in the visible and near IR by both mitochondrial and non-mitochondrial photoacceptors results in photobiomodulation, J. Photochem. Photobiol. B: Biol. 140 (2014) 344–358, http://dx.doi.org/10.1016/j.jphotobiol.2014.07.021.
[171] S.W. Ryter, R.M. Tyrrell, Singlet molecular oxygen ($^1O_2$): a possible effector of eukaryotic gene expression, Free Rad. Biol. Med. 24 (1998) 1520–1534, http://dx.doi.org/10.1016/S0891-5849(97)00461-9.
[172] R.M. Tyrrell, Modulation of gene expression by the oxidative stress generated in human skin cells by UVA radiation and the restoration of redox homeostasis, Photochem. Photobiol. Sci. 11 (2012) 135–147, http://dx.doi.org/10.1039/C1PP05222E.
[173] I.R. Sil´dos, L.A. Rebane, A.B. Treshchalov, A.É. Lykhmus, Luminescence of pairs of laser-excited oxygen molecules, JETP Lett. 22 (1975) 151–152.
[174] G.W. Koroll, A. Singh, Use of a high intensity dye laser to produce singlet oxygen, Photochem. Photobiol. 28 (1978) 611–613, http://dx.doi.org/10.1111/j.1751-1097.1978.tb06979.x.
[175] E. Furui, N. Akai, A. Ida, A. Kawai, K. Shibuya, Observation of collision-induced near-IR emission of singlet oxygen O_2 $a^1\Delta_g$ generated by visible light excitation of gaseous O_2 dimol, Chem. Phys. Lett. 471 (2009) 45–49, http://dx.doi.org/10.1016/j.cplett.2009.02.020.
[176] A. Ida, E. Furui, N. Akai, A. Kawai, K. Shibuya, Kinetic study on the photoabsorption process of gaseous O_2 dimol at 630 nm in a wide pressure range, Chem. Phys. Lett. 488 (2010) 130–134, http://dx.doi.org/10.1016/j.cplett.2010.02.022.
[177] A. Dube, C. Bock, E. Bauer, R. Kohli, P.K. Gupta, et al., He-Ne laser irradiation protects B-lymphoblasts from UVA-induced DNA damage, Radiat. Environ. Biophys. 40 (2001) 77–82, http://dx.doi.org/10.1007/s004110000086.
[178] W.P. Hu, J.J. Wang, C.L. Yu, C.C.E. Lan, G.S. Chen, et al., Helium–neon laser irradiation stimulates cell proliferation through photostimulatory effects in mitochondria, J. Invest. Dermatol. 127 (2007) 2048–2057, http://dx.doi.org/10.1038/sj.jid.5700826.
[179] T. Kushibiki, T. Hirasawa, S. Okawa, M. Ishihara, Regulation of miRNA expression by Low-Level Laser Therapy (LLLT) and Photodynamic Therapy (PDT), Int. J. Mol. Sci. 14 (2013) 13542–13558, http://dx.doi.org/10.3390/ijms140713542.
[180] A.V. Ivanov, A.A. Mashalov, S.D. Zakharov, Radioprotective action of low-intensity light into the red absorption band of endogenous molecular oxygen, J. Phys.: Conf. Ser. 740 (2016) 012014, http://dx.doi.org/10.1088/1742-6596/740/1/012014.
[181] S. Wu, F. Zhou, Y. Wei, W.R. Chen, Q. Chen, et al., Cancer phototherapy via selective photoinactivation of respiratory chain oxidase to trigger a fatal superoxide anion burst, Antioxid. Redox Signal. 20 (2014) 733–746, http://dx.doi.org/10.1089/ars.2013.5229.
[182] H. Chung, T. Dai, S.K. Sharma, Y.Y. Huang, J.D. Carroll, et al., The nuts and bolts of low-level laser (light) therapy, Ann. Biomed. Eng. 40 (2012) 516–533, http://dx.doi.org/10.1007/s10439-011-0454-7.
[183] M. Sneep, D. Ityaksov, I. Aben, H. Linnartz, W. Ubachs, Temperature-dependent cross sections of O_2–O_2 collision-induced absorption resonances at 477 and 577 nm, J. Quant. Spectrosc. Rad. Trans. 98 (2006) 405–424, http://dx.doi.org/10.1016/j.jqsrt.2005.06.004.
[184] M.J.C. Van Gemert, A.J. Welch, J.W. Pickering, O.T. Tan, G.H.M. Gijsbers, Wavelengths for laser treatment of port wine stains and telangiectasia, Lasers Surg. Med. 16 (1995) 147–155, http://dx.doi.org/10.1002/lsm.1900160204.
[185] A.V. Armichev, A.V. Ivanov, N.A. Panasenko, S.N. Perov, S.D. Zakharov, Spectral dependence of erythrocyte response to low-intensity irradiation at 570–590 nm, J. Rus. Laser Res. 16 (1995) 186–187, http://dx.doi.org/10.1007/BF02580877.
[186] H. Naus, W. Ubachs, The $b_g^{1\Sigma+} - X^{3\Sigma-}{}_g$ (3, 0) band of $^{16}O_2$ and $^{18}O_2$, J. Mol. Spectrosc. 193 (1999) 442–445, http://dx.doi.org/10.1006/jmsp.1998.7766.
[187] K.S. Kalogerakis, R.A. Copeland, T.G. Slanger, Collisional removal of O_2 ($b\ ^{1\Sigma+}{}_g$, v = 2,3), J. Chem. Phys. 116 (2002) 4877–4885, http://dx.doi.org/10.1063/1.1456026.
[188] A. Vogel, J. Noack, G. Hüttman, G. Paltauf, Mechanisms of femtosecond laser nanosurgery of cells and tissues, Appl. Phys. B 81 (2005) 1015–1047, http://dx.doi.org/10.1007/s00340-005-2036-6.
[189] S.D. Zakharov, I.M. Korochkin, A.S. Yusupov, V.V. Bezotosnyi, E.A. Cheshev, Application of diode lasers in light-oxygen cancer therapy, Semiconductors 48 (2014) 123–128, http://dx.doi.org/10.1134/S1063782614010254.
[190] W. Wai-Ying Kam, R.B. Banati, Effects of ionizing radiation on mitochondria, Free Radic. Biol. Med. 65 (2013) 607–619, http://dx.doi.org/10.1016/j.freeradbiomed.2013.07.024.
[191] D.B. Zorov, M. Juhaszova, S.J. Sollott, Mitochondrial reactive oxygen species (ROS) and ROS-induced ROS release, Physiol. Rev. 94 (2014) 909–950, http://dx.doi.org/10.1152/physrev.00026.2013.
[192] N.A. Graham, M. Tahmasian, B. Kohli, E. Komisopoulou, M. Zhu, et al., Glucose deprivation activates a metabolic and signaling amplification loop leading to cell death, Mol. Syst. Biol. 8 (2012) 589, http://dx.doi.org/10.1038/msb.2012.20.
[193] X. Zhou, Y. Wang, J. Si, R. Zhou, L. Gan, et al., Laser controlled singlet oxygen generation in mitochondria to promote mitochondrial DNA replication *in vitro*, Sci. Rep. 5 (2015) 16925, http://dx.doi.org/10.1038/srep16925.
[194] X. Zhou, Y. Wang, J. Si, R. Zhou, L. Gan, et al., Laser controlled singlet oxygen generation in mitochondria to promote mitochondrial DNA replication *in vitro*, Sci. Rep. 5 (2015) 16925, http://dx.doi.org/10.1038/srep16925.
[195] A. Prasad, U. Ferretti, M. Sedlářova, P. Pospíšil, Singlet oxygen production in *Chlamydomonas reinhardtii* under heat stress, Sci. Rep. 6 (2016) 20094, http://dx.doi.org/10.1038/srep20094.
[196] N. Rubio, S.P. Fleury, R.W. Redmond, Spatial and temporal dynamics of in vitro photodynamic cell killing: extracellular hydrogen peroxide mediates neighbouring cell death, Photochem. Photobiol. Sci. 8 (2009) 457–464, http://dx.doi.org/10.1039/B815343D.
[197] A. Chakraborty, K.D. Held, K.M. Prise, H.L. Liber, R.W. Redmond, Bystander effects induced by diffusing mediators after photodynamic stress, Rad. Res. 172 (2009) 74–81, http://dx.doi.org/10.1667/RR1669.1.
[198] I.A. Blair, Lipid hydroperoxides-mediated DNA damage, Exp. Geront. 36 (2001) 1473–1481, http://dx.doi.org/10.1016/S0531-5565(01)00133-4.
[199] N. Zarkovic, Z. Ilic, M. Jurin, R.J. Schaur, H. Puhl, et al., Stimulation of HeLa cell growth by physiological concentrations of 4-hydroxynonenal, Cell Biochem. Func. 11 (1993) 279–286, http://dx.doi.org/10.1002/cbf.290110409.
[200] S. Dwivedi, A. Sharma, B. Patrick, R. Sharma, Y.C. Awasthi, Role of 4-hydroxynonenal and its metabolites in signaling, Redox Report. 12 (2007) 4–10, http://dx.doi.org/10.1179/135100007×162211.
[201] E.E. Dubinina, V.A. Dadali, Role of 4-hydroxy-*trans*-2-nonenal in cell functions, Biochem. (Mosc.) 75 (2010) 1069–1087, http://dx.doi.org/10.1134/S0006297910090014.
[202] K.V. Ramana, A. Bhatnagar, S. Srivastava, U.C. Yadav, S. Awasthi, et al., Mitogenic responses of vascular smooth muscle cells to lipid peroxidation-derived aldehyde 4-hydroxy-trans-2-nonenal (HNE), J. Biol. Chem. 281 (2006) 17652–17660, http://dx.doi.org/10.1074/jbc.M600270200.
[203] K. Dittmann, C. Mayer, R. Kehlbach, M.C. Rothmund, H.P. Rodemann, Radiation-induced lipid peroxidation activates src kinase and triggers nuclear EGFR transport, Radiother. Oncol. 92 (2009) 379–382, http://dx.doi.org/10.1016/j.radonc.2009.06.003.
[204] H. Zhang, H.J. Forman, 4-Hydroxynonenal activates Src through a non-canonical pathway that involves EGFR/PTP1B, Free Rad. Biol. Med. 89 (2015) 701–707, http://dx.doi.org/10.1016/j.freeradbiomed.2015.08.025.
[205] Y.C. Awasthi, Y. Yang, N.K. Tiwari, B. Patrick, A. Sharma, et al., Regulation of 4-hydroxynonenal-mediated signaling by glutathione S-transferases, Free Rad. Biol. Med. 37 (2004) 607–619, http://dx.doi.org/10.1016/j.freeradbiomed.2004.05.033.
[206] W.G. Li, L.L. Stoll, J.B. Rice, S.P. Xu, F.J. Miller, et al., Activation of NAD(P)H oxidase by lipid hydroperoxides: mechanism of oxidant-mediated smooth muscle cytotoxicity, Free Rad. Biol. Med. 34 (2003) 937–946, http://dx.doi.org/10.1016/S0891-5849(03)00032-7.
[207] V. Mallikarjun, D.J. Clarke, C.J. Campbell, Cellular redox potential and the biomolecular electrochemical series: a systems hypothesis, Free Rad. Biol. Med. 53 (2012) 280–288, http://dx.doi.org/10.1016/j.freeradbiomed.2012.04.034.
[208] K.M. Holmström, T. Finkel, Cellular mechanisms and physiological consequences of redox-dependent signaling, Nat. Rev. Mol. Cell Biol. 15 (2014) 411–421, http://dx.doi.org/10.1038/nrm3801.
[209] A. Blázquez-Castro, J.C. Stockert, *In vitro* human cell responses to a low-dose photodynamic treatment vs. mild H_2O_2 exposure, J. Photochem. Photobiol. B: Biol. 143 (2015) 12–19, http://dx.doi.org/10.1016/j.jphotobiol.2014.12.015.
[210] D.P. Jones, Redox sensing: orthogonal control in cell cycle and apoptosis signalling, J. Intern. Med. 268 (2010) 432–448, http://dx.doi.org/10.1111/j.1365-2796.2010.02268.x.
[211] A. Gollmer, F. Besostri, T. Breitenbach, P.R. Ogilby, Spatially resolved two-photon irradiation of an intracellular singlet oxygen photosensitizer: correlating cell response to the site of localized irradiation, Free Rad. Res. 47 (2013) 718–730, http://dx.doi.org/10.3109/10715762.2013.817670.
[212] F. Perakis, L. De Marco, A. Shalit, F. Tang, Z.R. Kann, et al., Vibrational spectroscopy and dynamics of water, Chem. Rev. 116 (2016) 7590–7607, http://dx.doi.org/10.1021/acs.chemrev.5b00640.
[213] I.V. Bagrov, I.M. Belousova, V.M. Kiselev, I.M. Kislyakov, E.N. Sosnov, Observation of the Luminescence of Singlet Oxygen at λ = 1270 nm under LED Irradiation of CCl_4, Opt. Spectrosc. 113 (2012) 57–62, http://dx.doi.org/10.1134/S0030400×1207003X.
[214] I.V. Bagrov, V.M. Kiselev, I.M. Kislyakov, E.N. Sosnov, Direct optical excitation of singlet oxygen in organic solvents, Opt. Spectrosc. 116 (2014) 567–574, http://dx.doi.org/10.1134/S0030400×14040043.
[215] V.M. Kiselev, I.M. Kislyakov, I.V. Bagrov, Spectral dependence of the efficiency of direct optical excitation of molecular oxygen in tetrachloromethane, Opt. Spectrosc. 120 (2016) 859–863, http://dx.doi.org/10.1134/S0030400×16060114.

[216] W.R. Zipfel, R.M. Williams, W.W. Webb, Nonlinear magic: multiphoton microscopy in the biosciences, Nat. Biotech. 21 (2003) 1369–1377, http://dx.doi.org/10.1038/nbt899.
[217] E.E. Hoover, J.A. Squier, Advances in multiphoton microscopy technology, Nat. Phot. 7 (2013) 93–101, http://dx.doi.org/10.1038/NPHOTON.2013.361.
[218] S.D. Zakharov, N.C. Thanh, Photogenerated Singlet Oxygen Damages Cells in Optical Traps, 2009arXiv0911.4651T, 2009.
[219] M.K. Kuimova, S.W. Botchway, A.W. Parker, M. Balaz, H.A. Collins, et al., Imaging intracellular viscosity of a single cell during photoinduced cell death, Nat. Chem. 1 (2009) 69–73, http://dx.doi.org/10.1038/nchem.120.
[220] Y. Liu, D.K. Cheng, G.J. Sonek, M.W. Berns, C.F. Chapman, et al., Evidence for localized cell heating induced by infrared optical tweezers, Biophys. J. 68 (1995) 2137–2144, http://dx.doi.org/10.1016/S0006-3495(95)80396-6.
[221] A. Schönle, S.W. Hell, Heating by absorption in the focus of an objective lens, Opt. Lett. 23 (1998) 325–327, http://dx.doi.org/10.1364/OL.23.000325.
[222] E.J.G. Peterman, F. Gittes, C.F. Schmidt, Laser-Induced Heating in Optical Traps, Biophys. J. 84 (2003) 1308–1316, http://dx.doi.org/10.1016/S0006-3495(03)74946-7.
[223] C. Dressler, J. Beuthan, G. Mueller, U. Zabarylo, O. Minet, Fluorescence imaging of heat-stress induced mitochondrial long-term depolarization in breast cancer cells, J. Fluoresc. 16 (2006) 689–695, http://dx.doi.org/10.1007/s10895-006-0110-z.
[224] R. Zukiene, Z. Nauciene, J. Ciapaite, V. Mildažienė, Acute temperature resistance threshold in heart mitochondria: febrile temperature activates function but exceeding it collapses the membrane barrier, Int. J. Hyperth. 26 (2010) 56–66, http://dx.doi.org/10.3109/02656730903262140.
[225] M.G. White, O. Saleh, D. Nonner, E.F. Barrett, C.T. Moraes, et al., Mitochondrial dysfunction induced by heat stress in cultured rat CNS neurons, J. Neurophysiol. 108 (2012) 2203–2214, http://dx.doi.org/10.1152/jn.00638.2011.
[226] B. Crisan, O. Soritau, M. Baciut, R. Campian, L. Crisan, et al., Influence of different lasers wavelengths on nanoparticles components of human fibroblasts, Part. Sci. Tech. 31 (2013) 168–173, http://dx.doi.org/10.1080/02726351.2012.675019.
[227] Z. Wang, F. Cai, X. Chen, M. Luo, L. Hu, et al., The role of mitochondria-derived reactive oxygen species in hyperthermia-induced platelet apoptosis, PLoS One 8 (2013) e75044, http://dx.doi.org/10.1371/journal.pone.0075044.
[228] I.B. Slimen, T. Najar, A. Ghram, H. Dabbebi, M.B. Mrad, et al., Reactive oxygen species, heat stress and oxidative-induced mitochondrial damage. A review, Int. J. Hyperth. 30 (2014) 513–523, http://dx.doi.org/10.3109/02656736.2014.971446.
[229] M. Kikusato, H. Yoshida, K. Furukawa, M. Toyomizu, Effect of heat stress-induced production of mitochondrial reactive oxygen species on NADPH oxidase and hemeoxygenase-1 mRNA levels in avian muscle cells, J. Therm. Biol. 52 (2015) 8–13, http://dx.doi.org/10.1016/j.jtherbio.2015.04.005.
[230] I. Khan, E. Tang, P. Arany, Molecular pathway of near-infrared laser phototoxicity involves ATF-4 orchestrated ER stress, Sci. Rep. 5 (2015) 10581, http://dx.doi.org/10.1038/srep10581.